

**Multisite phosphorylation is required for sustained interaction with GRKs and arrestins in mediating rapid mu-opioid receptor desensitization.**

Elke Miess<sup>1#</sup>, Arisbel B Gondin<sup>2#</sup>, Arsalan Yousuf<sup>3#</sup>, Ralph Steinborn<sup>1</sup>, Nadja Mösslein<sup>4</sup>, Yunshi Yang<sup>4</sup>, Martin Göldner<sup>4</sup>, Julia G Ruland<sup>4</sup>, Moritz Bünemann<sup>4</sup>, Cornelius Krasel<sup>4</sup>, MacDonald J Christie<sup>3</sup>, Michelle L Halls<sup>2</sup>, Stefan Schulz<sup>1\*</sup> and Meritxell Canals<sup>2\*</sup>

<sup>1</sup>Department of Pharmacology and Toxicology, Jena University Hospital - Friedrich Schiller University Jena, Germany

<sup>2</sup>Drug Discovery Biology Theme, Monash Institute of Pharmaceutical Sciences, Monash University, Melbourne, Australia

<sup>3</sup> Discipline of Pharmacology, University of Sydney, Sydney, Australia

<sup>4</sup> Department of Pharmacology and Toxicology, Philipps-University Marburg, Germany

# These authors contributed equally to this work.

\* **Corresponding Authors:** Stefan Schulz, Ph.D., Institute of Pharmacology and Toxicology, Jena University Hospital - Friedrich Schiller University Jena, Drackendorfer Straße 1, D-07747 Jena, Germany, Phone: +49-3641-9325650, FAX: +49-3641-9325652, Email: [Stefan.Schulz@med.uni-jena.de](mailto:Stefan.Schulz@med.uni-jena.de); Meritxell Canals, Ph.D., Monash Institute of Pharmaceutical Sciences, 381 Royal Parade, Parkville, VIC 3052, Australia, Phone +61-3-99039094, Email: [meri.canals@monash.edu](mailto:meri.canals@monash.edu)

**Key Words:** G protein-coupled receptor, mu-opioid receptor,  $\beta$ -arrestin, GRK, internalization, phosphorylation, desensitization.

## ABSTRACT

G protein receptor kinases (GRKs) and  $\beta$ -arrestins are key regulators of  $\mu$ -opioid receptor (MOP) signaling and trafficking. We have previously shown that high-efficacy opioids such as DAMGO stimulate a GRK2/3-mediated multisite phosphorylation of conserved C-tail Ser and Thr residues, which facilitate internalization of the receptor. In contrast, morphine-induced phosphorylation is limited to Ser<sup>375</sup> and it is not sufficient to drive substantial receptor internalization. Here, we report how specific multisite phosphorylation controls the dynamics of GRK and  $\beta$ -arrestin interactions with MOP and show how such phosphorylation mediates receptor desensitization. We show that the kinetics of GRK2/3 recruitment to a DAMGO-activated MOP are faster than the kinetics of  $\beta$ -arrestin recruitment.  $\beta$ -arrestin recruitment requires GRK2 activity and MOP phosphorylation, but surprisingly, GRK recruitment is also dependent on the integrity of the phosphorylation sites in the C-terminus. Translocation of both regulatory proteins and their stable interaction with MOP are dependent on phosphorylation of four Ser and Thr residues within the <sup>370</sup>TREHPSTANT<sup>379</sup> motif of the C-tail. Our results also suggest that other residues outside this motif participate in the initial and transient recruitment of GRK and  $\beta$ -arrestins. Finally, using complementary patch clamp approaches, we show that high efficacy agonist desensitization of MOP has two components; a sustained component, which requires GRK2-mediated phosphorylation and a potential soluble factor, and a rapid component likely mediated by GRK2 but independent of receptor phosphorylation. Elucidating these complex receptor-effector interactions represents an important step towards a mechanistic understanding of MOP desensitization that leads to the development of tolerance and dependence.

## INTRODUCTION

Opioids such as morphine are still the mainstay analgesics for the treatment of severe pain. However, the development of tolerance, addiction and respiratory depression severely limits their utility (1). These unwanted effects of opioids are key contributors to opioid-induced overdose deaths, which have drastically increased in the last decade (2).

The  $\mu$ -opioid receptor (MOP) is the G protein-coupled receptor (GPCR) targeted by morphine and most opioid analgesics (3). Since the initial observation that morphine elicited less tolerance and decreased side effects in mice lacking  $\beta$ -arrestin2 (4, 5), substantial efforts have focused on the development of opioid ligands that preferentially activate G protein-mediated signals over  $\beta$ -arrestin recruitment. These efforts have resulted in the discovery of several molecules with an improved side effect profile and increased therapeutic window (6-8). However, the cellular mechanisms whereby opioids mediate analgesia vs other side effects are far from clear. MOP desensitization is considered to be the initial step for the development of tolerance. Such desensitization entails phosphorylation of the receptor, recruitment of regulatory proteins such as  $\beta$ -arrestins and receptor internalization (1). Together, these regulatory processes result in a reduction of opioid response or sensitivity.

The ligand-dependent and hierarchical nature of MOP phosphorylation and its role in MOP desensitization and internalization has been previously established. Quantitative mass spectrometry and phosphorylation site-specific antibodies have identified two clusters of MOP residues, <sup>354</sup>TSST<sup>357</sup> and <sup>370</sup>TREHPSTANT<sup>379</sup> within its C-terminal region, that undergo opioid-induced phosphorylation (9-11). Agonist-mediated phosphorylation of MOP is initiated at Ser<sup>375</sup>, but it is the ability of such agonists to induce higher order phosphorylation on flanking residues that dictates their propensity to internalize MOP. Different opioids produce different phosphorylation patterns; multisite phosphorylation in the C-terminal region of MOP occurs

robustly for agonists that induce internalization with less phosphorylation of fewer sites for those that do not (9-11).

Rapid desensitization of MOP coupling to membrane effectors such as voltage-gated calcium channels (VGCCs) and inwardly rectifying K channels (GIRKs; Kir3.X) also precedes internalization, but its relationship to phosphorylation events and  $\beta$ -arrestin recruitment remains unclear (1, 12). We have previously shown that C-terminal phosphorylation of MOP is necessary for some forms of desensitization, but that this effect is also ligand dependent (13). Mutation of all Ser and Thr residues within the C-terminal tail of MOP completely abolished [Met<sup>5</sup>]-enkephalin (ME)-, but not morphine-, induced desensitization. In vivo, introduction of a S375A mutation in transgenic mice diminished the development of tolerance to high-efficacy opioid agonists such as DAMGO or etonitazene, while tolerance to chronic morphine appeared unaffected (14). Compound 101 (Cmpd101), a small molecule inhibitor that prevents G protein receptor kinase (GRK) 2/3 activation (15), only partially blocked ME-, DAMGO- and morphine-induced MOR desensitization of GIRKs in rat and mouse locus coeruleus neurons (16), suggesting GRK2/3-independent mechanisms of MOP desensitization.

It is now clear that multisite phosphorylation of MOP induced by high intrinsic efficacy agonists such as DAMGO or ME requires GRK2/3 (11), and that activation of MOP by these ligands results in  $\beta$ -arrestin recruitment to the receptor (17-19). Overexpression of GRK2 also facilitates morphine-induced  $\beta$ -arrestin recruitment and MOP internalization (20), supporting a key role of this kinase in MOP regulation. However, it is still unknown what dictates GRK-MOP interactions. Moreover, Raveh et al. (21) have proposed that GRKs may act to desensitize GIRK channels via a mechanism that is independent of their kinase activity through competition for the  $\beta\gamma$  subunits of the G protein that activate these channels.

It is thus clear that GRKs and arrestins are critical regulatory proteins for which interaction with

MOP prior to internalization has major implications for opioid signaling. However, the molecular determinants that control these interactions are still elusive. How phosphorylation regulates these interactions and what relevance this has for MOP desensitization are questions that remain to be addressed.

In the present study, we report a systematic assessment of how specific multisite phosphorylation controls the dynamics of GRK and  $\beta$ -arrestin interactions with MOP and show how such phosphorylation mediates receptor desensitization. Using Bioluminescence and Förster Resonance Energy Transfer (BRET and FRET) as well as  $\beta$ -galactosidase ( $\beta$ -Gal) complementation technology, we show that the kinetics of GRK2/3 recruitment to a DAMGO-activated MOP are faster than the kinetics of  $\beta$ -arrestin recruitment.  $\beta$ -arrestin recruitment requires GRK2 activity and MOP phosphorylation, but surprisingly, GRK recruitment is also dependent on the integrity of the phosphorylation sites in the C-terminus of MOP. While the <sup>370</sup>TREHPSTANT<sup>379</sup> motif is required for effective recruitment of GRKs and  $\beta$ -arrestins, the <sup>354</sup>TSST<sup>357</sup> region participates in the long-term stability of such interactions. Interestingly, both GRKs and  $\beta$ -arrestins show residual recruitment to a mutant receptor with all C-terminal phosphosites mutated. Finally, using complementary patch clamp approaches, we unravel a fast desensitization event that is independent of MOP phosphorylation as well as a sustained desensitization component, which requires GRK2-mediated phosphorylation of the <sup>370</sup>TREHPSTANT<sup>379</sup> motif and a potential soluble factor. Elucidating these complex receptor-effector interactions represents an important step towards a mechanistic understanding of MOP desensitization that leads to the development of tolerance and dependence.

## RESULTS

### Agonist-dependent recruitment of $\beta$ -arrestins to wild-type MOP

We have recently developed complementary approaches that allow for the systematic investigation of the dynamics and mechanisms of  $\beta$ -arrestin recruitment to MOP. FRET and BRET allow the real-time assessment of the recruitment of a fluorescently tagged  $\beta$ -arrestin (CFP or YFP, respectively) to a C-terminally tagged MOP (YFP or RLuc8, respectively). In addition, we have also developed a  $\beta$ -galactosidase ( $\beta$ -Gal) complementation approach to measure steady-state interactions between  $\beta$ -arrestin and MOP. Thus, while FRET and BRET provide information about the dynamics of  $\beta$ -arrestin recruitment at early time points, the  $\beta$ -Gal complementation assay provides further insight into the stability of these interactions (Figure 1A).

The high intrinsic efficacy agonist DAMGO and the low intrinsic efficacy opiate morphine (both at  $1\mu\text{M}$ ) increased the BRET signal between MOP-RLuc8 and  $\beta$ -arrestin2-YFP to reach a maximum within 1 min, although the signal obtained with morphine was smaller than that obtained with DAMGO (Figure 1B). Importantly, this signal was blocked by addition of the antagonist naloxone ( $30\mu\text{M}$ ), showing specificity and reversibility of the response (Figure 1B). FRET measurements between MOP-YFP and  $\beta$ -arrestin2-CFP showed similar results (Figure 1C) (22). Activation of MOP with saturating concentrations of DAMGO ( $10\mu\text{M}$ ) promoted  $\beta$ -arrestin2 recruitment to the receptor that reached its maximal signal within 1 min and was reversed after agonist removal. Saturating concentrations of morphine ( $30\mu\text{M}$ ) also induced  $\beta$ -arrestin2-CFP recruitment to MOP-YFP, although with a lower FRET signal (Figure 1C).

We then constructed concentration-response curves for  $\beta$ -arrestin1 and  $\beta$ -arrestin2 recruitment using BRET (10 min incubation) or  $\beta$ -Gal complementation assays (1 h incubation) (Figure 1D-G). DAMGO induced a concentration-dependent recruitment of  $\beta$ -arrestin1 and  $\beta$ -arrestin2 in both assays with similar potencies (Table 1). In contrast, morphine did not significantly induce  $\beta$ -

arrestin1 recruitment, and caused only a partial recruitment of  $\beta$ -arrestin2 with similar potency as DAMGO (Table 1). These results are in agreement with previous findings that show a compromised ability of morphine to recruit  $\beta$ -arrestins in the absence of GRK overexpression (18, 20).

### **Recruitment of $\beta$ -arrestins to phosphorylation-deficient MOP mutants**

To map putative phosphate acceptor sites controlling MOP phosphorylation, we generated phosphorylation-deficient MOP mutants and directly assessed the correlation between phosphorylation and recruitment of regulatory proteins. Receptor phosphorylation at candidate sites was evaluated using phosphosite-specific antibodies (Figure 2A). Mutations of Ser and Thr (S/T) residues to alanine (A) in different regions of wild-type (WT) MOP generated the following phosphorylation-deficient MOP mutants: TSST-4A (mutations in the <sup>354</sup>TSST<sup>357</sup> cluster), S375A (mutation of Ser<sup>375</sup>), STANT-3A (mutations in the <sup>375</sup>STANT<sup>379</sup> cluster), TREHPSTANT-4A (mutations in the <sup>370</sup>TREHPSTANT<sup>379</sup> motif) and 11S/T-A (mutation of all 11 potential C-terminal S/T phosphorylation sites) (Figure 2A).

Consistent with earlier observations, no constitutive phosphorylation of Ser<sup>356</sup>/Thr<sup>357</sup>, Thr<sup>370</sup>, Ser<sup>375</sup>, Thr<sup>376</sup> or Thr<sup>379</sup> was observed. Agonist stimulation with morphine resulted in phosphorylation of Ser<sup>375</sup> and only induced weak phosphorylation of the Thr<sup>370</sup>, Thr<sup>376</sup> and Thr<sup>379</sup> residues. In contrast, DAMGO resulted in robust MOP phosphorylation at all the sites contained within <sup>370</sup>TREHPSTANT<sup>379</sup> domain (Figure 2B) (10, 11). Equivalent receptor loading was confirmed by detecting a distinct non-phosphorylated epitope in the cytoplasmic tail.

Expanding from previous studies, we generated a phosphosite-specific antiserum against Ser<sup>356</sup> and Thr<sup>357</sup> of the <sup>354</sup>TSST<sup>357</sup> motif of the MOP C-terminal tail (pS356/pT357). DAMGO stimulation induced very weak phosphorylation of these residues, which was abolished in the TSST-4A mutant. Morphine did not promote any phosphorylation of these residues (Figure 2B). In addition,

mutation of the <sup>354</sup>TSST<sup>357</sup> motif in the TSST-4A mutant produced a modest decrease in the phosphorylation at other S/T sites by both ligands. This excludes both Ser<sup>356</sup>/Thr<sup>357</sup> as prominent initial sites for agonist-induced MOP phosphorylation but highlights that the integrity of the <sup>354</sup>TSST<sup>357</sup> cluster might be important for regulatory events that depend on robust phosphorylation within the <sup>370</sup>TREHPSTANT<sup>379</sup> domain.

Point mutation of Ser<sup>375</sup> (S375A mutant) within the <sup>375</sup>STANT<sup>379</sup> motif, prevented detectable phosphorylation at Ser<sup>356</sup>/Thr<sup>357</sup>, Thr<sup>376</sup> and Thr<sup>379</sup>, and also significantly reduced phosphorylation at Thr<sup>370</sup> (Figure 2B). This confirms Ser<sup>375</sup> as the initial residue for agonist-specific hierarchical MOP phosphorylation as previously reported (10, 11). As expected, detection of phosphorylated MOP by any of the phospho-specific antibodies was blocked by mutation of the <sup>370</sup>TREHPSTANT<sup>379</sup> motif or mutation of all S/T residues in the cytoplasmic tail (11S/T-A mutant) (Figure 2B).

To directly assess the relationship between receptor phosphorylation and the recruitment of  $\beta$ -arrestin1/2, we generated phosphorylation-deficient MOP mutants (Figure 2A) suitable for BRET, FRET and  $\beta$ -Gal complementation assay. Correct expression and function of these mutants was evaluated by anti-FLAG ELISA and inhibition of forskolin-induced cAMP of FLAG-tagged MOP constructs without C-terminal tags (Supplemental Figure 1, Supplemental Table 1).

Mutation of the <sup>354</sup>TSST<sup>357</sup> cluster (TSST-4A) had no effect on DAMGO-induced  $\beta$ -arrestin1 or  $\beta$ -arrestin2 recruitment when measured using BRET (Figure 3A, B and C, Tables 2 and 3). However, when the interaction between  $\beta$ -arrestins and MOP was detected using  $\beta$ -Gal complementation, deletion of this cluster led to a significant decrease of absolute  $\beta$ -arrestin1 and  $\beta$ -arrestin2 recruitment ( $E_{max}$ ), while the potency of DAMGO remained unchanged (Figure 3B and C, Table 2 and 3).  $\beta$ -Gal complementation requires the two fragments to be in the correct relative orientation to form a functional enzyme, which has been suggested to occur upon “stable” interactions (30-90 min). In contrast, for FRET and BRET to occur, the relative orientation between

the receptor and  $\beta$ -arrestin is under fewer constraints. Thus, these data suggest that while the initial recruitment of  $\beta$ -arrestins to the receptor may not be affected by mutation of the <sup>354</sup>TSST<sup>357</sup> motif, the stability of this interaction is affected upon mutation of this motif to alanine. Thus, phosphorylation of the <sup>354</sup>TSST<sup>357</sup> region, although not directly involved in  $\beta$ -arrestin recruitment, may participate in the stability of the  $\beta$ -arrestin/MOP complex.

Mutation of the <sup>375</sup>STANT<sup>379</sup> cluster (STANT-3A) or <sup>370</sup>TREHPSTANT<sup>379</sup>, significantly affected DAMGO-induced  $\beta$ -arrestin1 and  $\beta$ -arrestin2 recruitment to MOP in both BRET and  $\beta$ -Gal complementation assays (Figure 3A-C), respectively. Although DAMGO's potency was unaffected in this mutant, there was a ~50% reduction of the maximal effect of this ligand (Table 2 and 3). These results suggest that the <sup>375</sup>STANT<sup>379</sup> motif plus Thr<sup>370</sup> are a key region for receptor-arrestin interactions, most likely participating in the initial recruitment of  $\beta$ -arrestin to the activated receptor. Within this region lies Ser<sup>375</sup>, which drives the hierarchical phosphorylation of MOP. Interestingly, single mutation of S375A affected the dynamics of  $\beta$ -arrestin2 recruitment. While the BRET response to DAMGO within the first 5 minutes after stimulation was similar to the WT receptor, the signal rapidly decayed to levels similar to those measured for the STANT-3A mutant (Figure 3A) and although the potency of DAMGO at this mutant was similar to that of the WT receptor, its maximal effect was reduced by 30% (Table 3). As expected, in the  $\beta$ -Gal complementation assay the recruitment induced by DAMGO at the MOP S375A was significantly affected (Figure 3B and C, Table 3). In addition, FRET experiments between MOP S375A-YFP and  $\beta$ -arrestin2-CFP also showed significant effects of this mutation on  $\beta$ -arrestin2 recruitment (Figure 3D). Together these results not only support the observations that phosphorylation of Ser<sup>375</sup> serves as an initial residue for multisite phosphorylation but also suggest that this site is key to prolonging the interaction between MOP and  $\beta$ -arrestins. Finally, we assessed  $\beta$ -arrestin2 recruitment to a mutant receptor where all the phosphorylation sites of the C-tail have been

mutated to alanine (11S/T-A). As expected, at this mutant DAMGO-induced  $\beta$ -arrestin1/2 recruitment was significantly compromised in all the three assays (Figure 3, Table 2 and 3).

Of note, we observed that although the DAMGO-induced BRET signal was dramatically reduced in the STANT-3A and 11S/T-A mutants, it was not completely abolished (i.e it still increased from basal levels upon addition of the agonist). Interestingly, addition of the antagonist naloxone (30 $\mu$ M) was able to completely reverse the BRET signal to basal levels (Supplemental Figure 2). A similar effect could also be observed in the FRET assay after agonist removal (Figure 3D), although recruitment of  $\beta$ -arrestin2 was not detected for the two phosphorylation-deficient mutants in the  $\beta$ -Gal complementation assay. These data suggest that even in the absence of phosphorylation sites in the C-tail of the MOP,  $\beta$ -arrestins can be transiently recruited to the receptor upon agonist stimulation.

We also investigated the effects of the above mutations on morphine-induced  $\beta$ -arrestin2 recruitment. As observed in the WT receptor, the response induced by morphine was significantly weaker than that induced by DAMGO (Figure 3A, Table 3). However, the effect of all mutations on morphine's effects mirrored those observed for the high efficacy agonist DAMGO.

As  $\beta$ -arrestin recruitment precedes MOP internalization (1), we assessed the ability of DAMGO to promote endocytosis of MOP phospho-deficient mutants using BRET, cell-surface ELISA and confocal imaging. DAMGO stimulation of WT receptor (but not morphine stimulation) induced an increase of the BRET signal between MOP-RLuc8 and an early endosome resident protein (Rab5a-Venus) (Figure 4A). This was also observed in cell-surface ELISA assay, which quantifies agonist-induced reduction of cell surface receptor (Figure 4B). Confocal imaging of the HA-tagged MOP and phospho-deficient mutants (Supplemental Figure 1C) also confirmed these data. Mutations of <sup>354</sup>TSST<sup>357</sup> motif had a weak effect on DAMGO-induced MOP internalization (Figure 4A, B), however mutations S375A, STANT-3A, TREHPSTANT-4A or 11S/T-A severely impaired receptor endocytosis.

These results are in agreement with the  $\beta$ -arrestin recruitment data, and support the requirement of a strong and sustained MOP- $\beta$ -arrestin interaction to drive receptor internalization.

### **Role of GRKs in $\beta$ -arrestin recruitment**

Agonist-induced phosphorylation of MOP is mediated by GRKs. In particular, GRK2 and GRK3 are mainly involved in MOP phosphorylation upon stimulation with high-efficacy agonists, such as DAMGO (11). We thus investigated the influence of overexpression, knockdown and pharmacological inhibition of GRK2/3 on  $\beta$ -arrestin recruitment using BRET and  $\beta$ -Gal complementation approaches.

As expected, overexpression of GRK2/3 resulted in increased efficacy and potency of DAMGO- and morphine-induced  $\beta$ -arrestin1 (Supplemental Figure 3A) and  $\beta$ -arrestin2 recruitment in both assays (Figure 5A-D and Table 4). In addition, and extending previous studies that showed that GRK2 overexpression increases Ser<sup>375</sup> phosphorylation by morphine, we show that GRK2/3 overexpression facilitates morphine-induced multiphosphorylation at Thr<sup>370</sup> and Thr<sup>379</sup> contained within the <sup>370</sup>TREHPSTANT<sup>379</sup> motif (Figure 5E). Depletion of endogenous GRK2 or GRK3 alone by siRNA or by overexpression of a catalytically inactive GRK2 (GRK2 K220R, GRK2-DN) had a small effect in reducing the efficacy of DAMGO and morphine to recruit  $\beta$ -arrestin2 (Figure 5A and F, Table 4). Inhibition by a specific inhibitor of GRK2/3, Compound 101 (Cmpd101) (15), resulted in inhibition of DAMGO-induced  $\beta$ -arrestin2 recruitment (Figure 5G). Finally, the effect of GRK2 expression levels and activity on MOP internalization was evaluated using BRET between MOP-RLuc8 and Rab5a-Venus. In agreement with the  $\beta$ -arrestin recruitment data and with previous reports, MOP internalization in response to both DAMGO and morphine was enhanced by GRK2 overexpression and abolished by incubation with Cmpd101 (Supplemental Figure 3B). Together these results illustrate the key role of GRK2/3 in the recruitment of  $\beta$ -arrestins and receptor endocytosis induced by opioid agonists.

## GRK recruitment to activated wild type and phosphorylation-deficient MOP mutants

To understand the dynamics and mechanisms of GRK recruitment to MOP, we developed FRET, BRET and  $\beta$ -Gal complementation approaches with the same donor-acceptor pairs used in the  $\beta$ -arrestin assays described above. Real time measurements of FRET between MOP-YFP and GRK2-mTurquoise or BRET between MOP-RLuc8 and GRK2-Venus showed that GRK2 recruitment to the activated receptor occurs faster than  $\beta$ -arrestin translocation (half time  $[t_{1/2}] = 2.3$  s for GRK2 FRET and  $t_{1/2} = 20$ s for GRK2 BRET vs  $t_{1/2} = 42$ s for  $\beta$ -arrestin2 FRET and  $t_{1/2} = 66$ s for  $\beta$ -arrestin2 BRET; Supplemental Figure 4) and reversed to basal upon agonist removal or addition of 30  $\mu$ M naloxone (Figure 6A and B). Concentration-response curves constructed using BRET or  $\beta$ -Gal complementation assays estimated a potency of 0.6  $\mu$ M for DAMGO and 0.43  $\mu$ M for morphine (Figure 6C and D, Table 5). Similar results were obtained for GRK3 in the  $\beta$ -Gal complementation assay (Supplemental Figure 4). Cmpd101 completely prevented GRK2 recruitment to activated MOP (Figure 6E) suggesting that an active GRK2 is required for its interaction with MOP.

We next sought to understand the role of phosphorylation within MOP C-tail on GRK2 translocation. We obtained similar results to the  $\beta$ -arrestin recruitment data described above. Namely, mutation of the <sup>354</sup>TSST<sup>357</sup> motif (TSST-4A) did not affect early BRET measurements (Figure 7A and B, Table 6) while it had a robust effect on GRK2 recruitment measured by  $\beta$ -Gal complementation (Figure 7C, Table 6). These results again suggest a role of this region in the stability of interactions between the receptor and regulatory proteins. Mutations S375A, STANT-3A and 11S/T-A all had a significant effect in reducing GRK2 recruitment in both assays (Figure 7A-C). Similar results were obtained for GRK3 in the  $\beta$ -Gal complementation assay (Supplemental Figure 4).

FRET experiments using the S375A and 11S/T-A mutants and GRK2-mTurquoise showed agonist-induced recruitment of GRK2 to phosphorylation-deficient mutants that was reversible after

agonist washout (Figure 7D). Again, it is interesting to note that, as with  $\beta$ -arrestin2 recruitment, although the BRET signal was dramatically reduced in the STANT-3A and 11ST/-A mutants, it was not completely abolished (i.e. it still increased from basal levels upon addition of the ligand) and only addition of the antagonist naloxone (30 $\mu$ M) was able to completely return the BRET signal to basal levels (Supplemental Figure 4). These data support the notion that even in the absence of phosphorylation sites at the C-tail of the MOP, GRKs and  $\beta$ -arrestins can be transiently recruited to the receptor upon agonist stimulation.

### **Desensitization of phosphorylation-deficient MOP mutants.**

Phosphorylation sites in the vicinity of <sup>354</sup>TSST<sup>357</sup> and <sup>375</sup>STANT<sup>379</sup> have been shown to play important roles in MOP desensitization. Using conventional whole cell mode of patch clamp recording, Birdsong *et al.* (2015) reported that STANT-3A mutation and, more substantially, STANT-3A plus TSST-4A impaired desensitization by ME in neurons (23). By contrast, using perforated patch clamp recording to limit disruption of the cytoplasmic milieu, we previously reported that mutation of 6 S/T residues, including STANT, abolished ME-induced internalization but did not inhibit desensitization and that impairment of ME-induced desensitization required mutation of all 11 S/T residues in the C-tail (13). We therefore compared desensitization of the STANT-3A and TSST-4A mutants using both whole cell and perforated patch clamp recording. As previously reported (13) an initial rapid component of GIRK desensitization (with a time constant of approximately 2-4 s) was observed upon application of ME (10 $\mu$ M) for both TSST-4A and STANT-3A mutants that was not significantly different from WT MOP (Supplemental Figure 5). This rapid component was not observed using a concentration of ME below 100nM and was less prominent during application of morphine than ME (10 $\mu$ M; Supplemental Figure 5). This most likely reflects GIRK regulation by GRK2 that is recruited to the receptor-channel complex by ME but less effectively by morphine, as suggested previously (21). However, it should be noted that

the potency of ME to induce this rapid desensitization component could not be resolved as the on-rate of ME activated  $G_{GIRK}$  overlaps substantially at low concentrations with the on-rate of the declining component (Supplemental Figure 5A).

Using perforated patch clamp, both STANT-3A and TSST-4A mutants showed acute desensitization upon exposure to supramaximal concentrations of both ME and morphine (10 $\mu$ M), similar to WT MOP (Figure 8A and D). An acute decline of GIRK conductance was observed during the 5 min exposure to both ME and morphine for both the mutants and WT. As previously reported, the decline in peak GIRK conductance is an insensitive measure of receptor desensitization because of the large receptor reserve present in these cells (13, 24). Desensitization of the response to a submaximal concentration of ME (10nM) was highly significant for TSST-4A, STANT-3A and WT MOP ( $P < 0.0001$  in each case; One sample t-test). Of note, and as previously reported (13), a smaller component of heterologous desensitization of responses to somatostatin acting on somatostatin receptors natively expressed in AtT20 cells was observed in all mutants (Supplemental Figure 5E). By contrast, desensitization by ME was significantly reduced under whole cell patch clamp recording in the STANT-3A mutant (77 $\pm$ 8 % in whole cell patch vs 19 $\pm$ 3% in perforated patch) but was maintained in TSST-4A and WT MOP (18 $\pm$ 3% for TSST-4A and 22 $\pm$ 5% for WT MOP, Figure 8B and E and Supplemental Figure 6). These results suggest that diffusion out of the cell of cytoplasmic desensitization mediators occurs during whole cell but not perforated patch clamp recording conditions.

We and others have previously reported that inhibition of protein kinase C (PKC) impairs MOP desensitization (13, 25). Moreover, we previously reported that PKC $\alpha$  caused restricted receptor mobility upon activation by morphine but not DAMGO (26). To assess the role of PKC, cells were pre-incubated with the PKC inhibitor, Calphostin C, and were exposed to the inhibitor throughout recordings. Calphostin C (30nM) did not affect desensitization by ME in WT or TSST-4A MOP but

significantly reduced ME induced desensitization of STANT-3A (Figure 8C and F). These data suggest that ME-induced desensitization by soluble mediators of the STANT-3A mutant is sensitive to PKC inhibition, in a similar manner as previously observed for morphine at the WT MOP (13).

## DISCUSSION

This study identifies the role of multisite phosphorylation of MOP in promoting receptor interactions with GRKs and  $\beta$ -arrestins and mediating rapid receptor desensitization. We have systematically mutated the 11 Ser and Thr residues present in the C-tail of MOP. The use of complementary approaches to measure protein-protein interactions permits the assessment of the dynamics of complex formation and provides key information about the roles that different C-terminal motifs play in such dynamic interactions.

The <sup>354</sup>TSST<sup>357</sup> cluster in the proximal region of the C-tail of MOP does not participate in receptor internalization (Figure 4) (9). However, Birdsong et al. identified the TSST region as a major mediator of the generation of the high-affinity state of the receptor upon high efficacy agonist stimulation, suggesting that phosphorylation of this motif can have an allosteric effect on ligand binding (23). Our data shows that although mutation of the <sup>354</sup>TSST<sup>357</sup> motif (TSST-4A) did not abolish phosphorylation, it did induce a detectable decrease in multisite phosphorylation induced by DAMGO (Figure 2). Interestingly, for this mutant, recruitment of GRK2/3 and  $\beta$ -arrestins within the first 30 min remained unaffected (Figures 3 and 7), whereas no detectable recruitment occurred after 1 h incubation, as observed using the  $\beta$ Gal complementation approach (Figures 3 and 7). Moreover, desensitization of TSST-4A MOP was indistinguishable from WT (Figure 8). Together, these results suggest that the TSST region, by allosterically modulating ligand binding, participates in the stability of the interaction of MOP with regulatory proteins but has no impact on MOP desensitization and internalization.

Our data support previous findings suggesting that Ser<sup>375</sup> serves as an initial residue that drives hierarchical multisite phosphorylation of MOP (11, 27). As we have previously described, single mutation of this residue severely compromised phosphorylation of other Ser and Thr residues (Figure 2B). Moreover, phosphorylation of Ser<sup>375</sup> had a significant impact on the dynamics of

recruitment of GRK2 and  $\beta$ -arrestin (Figures 3 and 7). S375A MOP was still able to recruit GRK2 and  $\beta$ -arrestin at early time points (5 min), however, the interaction of these proteins with the mutant receptor were very transient. We detected a steady decrease in the  $\beta$ -arrestin recruitment BRET signal after 5 min, and no detectable recruitment was observed after 1 h incubation (Figures 3 and 7). The use of complementary assays that rely on different stability constraints ( $\beta$ -Gal complementation vs FRET and BRET) has allowed for the detection of these different dynamics dictated by receptor phosphorylation. The compromised internalization of S375A also suggests that robust phosphorylation and stable interactions with GRK2 and  $\beta$ -arrestins are required to drive MOP endocytosis. Ser<sup>375</sup> is the first residue of the <sup>375</sup>STANT<sup>379</sup> motif. This region has previously been reported to play a key role in receptor internalization (9), although conflicting results have been reported regarding the ability of this mutant to desensitize (13, 23). In the present study we reconcile the differences observed with regards to the desensitization of this mutant (Figure 8). Our data clearly suggest that the <sup>375</sup>STANT<sup>379</sup> region is crucial for regulating MOP desensitization. High efficacy agonists like DAMGO and ME regulate MOP desensitization by a GRK2/ $\beta$ -arrestin-mediated mechanism upon phosphorylating crucial sites within this region. Moreover, the observation that the compromised desensitization of the STANT-3A mutant is only detectable when using whole cell patch clamp further suggests the requirement of a soluble (cytosolic) factor as a mediator of this desensitization. In agreement with this, we show that GRK2/3 and  $\beta$ -arrestin recruitment, as well as receptor internalization at STANT-3A MOP were severely compromised (Figures 3, 4 and 7). The key role of the <sup>375</sup>STANT<sup>379</sup> region in the regulation of MOP is also illustrated by the results obtained upon mutation of all Ser and Thr residues within the C-tail of MOP (11ST/A) (Figures 3, 4 and 7).

Due to its limited ability to induce multisite phosphorylation of MOP (Figure 2B), morphine induced very weak recruitment of  $\beta$ -arrestins (Figures 1 and 5). Overexpression of GRK2/3 facilitated phosphorylation of Thr<sup>370</sup> and Thr<sup>379</sup> (in addition to Ser<sup>375</sup>) by morphine, which resulted

in both increased  $\beta$ -arrestin recruitment and MOP internalization (Figure 5 and Supplemental Figure 3). These results highlight that the cellular effect of a particular ligand (in this case morphine) is highly dependent on the cellular context, and that differences in expression levels of signaling and regulatory proteins will influence the downstream events of receptor activation in a particular cell type. For example, different expression levels of GRK2 may explain why morphine internalizes MOP in striatal neurons (28) but not in other neurons (29), although this remains to be confirmed.

An important finding of the current study is that even when all Ser and Thr residues of the C-tail of MOP were mutated to Ala, we were able to detect GRK2 and  $\beta$ -arrestin recruitment using BRET and FRET approaches but not when using the  $\beta$ -Gal complementation assay. Importantly, these signals were abolished by addition of the antagonist naloxone or by agonist washout (Supplemental Figures 2 and 4). These results suggest that both GRK2 and  $\beta$ -arrestins can be transiently recruited to the activated MOP independently of receptor phosphorylation. Indeed, phosphorylation-independent recruitment of  $\beta$ -arrestins has been reported for several GPCRs (30, 31). Moreover, this recruitment of GRK2 is likely to mediate the rapid component of GIRK desensitization (21), which still occurred in the STANT-3A mutant (Supplemental Figure 5).

It is well established that GRKs play a key role in GPCR regulation, that they phosphorylate activated receptors, uncoupling them from G proteins and facilitating interactions with  $\beta$ -arrestins to promote alternative signaling and/or receptor endocytosis. Indeed our results show that GRK2 activity is required for efficient arrestin recruitment and MOP internalization (Figure 5 and Supplemental Figure 3). An unexpected result from our studies was that the interaction between GRK2 and the activated MOP also seemed to be dependent on the integrity of the phosphorylation sites (Figure 7). Cmpd101 prevented recruitment of GRK2 to the activated MOP, consequently compromising  $\beta$ -arrestin recruitment and receptor internalization. Binding of

Cmpd101 to GRK2 induces small conformational changes that stabilize GRK2 in a non-active, non-catalytic conformation (15). Thus, our results suggest that the unblocked conformation of GRK2/3 is required for the recruitment and interaction of this kinase with MOP.

Although the molecular mechanisms underlying the development of morphine-induced tolerance remain controversial, it is generally accepted that MOP desensitization of VGCC and GIRK channels is an important step. As mentioned above, our results suggest that MOP desensitization by high efficacy ligands has two components; a sustained component, which requires GRK2-mediated phosphorylation and a potential soluble factor, and a rapid component independent of receptor phosphorylation (Figure 8 and Supplemental Figure 5). This desensitization component, independent of kinase activity, highlights the potential dual role of GRKs, acting as scaffolding/sequestering proteins in addition to their kinase activity, as earlier suggested by Raveh et al. (21). In addition to GRKs, PKC has also been suggested to participate in the development of tolerance to morphine (25), although the molecular basis of this remains unclear. Our patch clamp studies suggest that in the STANT-3A MOP mutant, PKC becomes important in mediating ME desensitization (Figure 5). Whether PKC phosphorylates Ser<sup>363</sup> and/or Thr<sup>370</sup> as previously suggested (32, 33) or whether PKC is the soluble factor mediating sustained desensitization, remains to be investigated.

In summary our results demonstrate the complex role of MOP phosphorylation in receptor desensitization and in the recruitment of regulatory and scaffolding proteins. These receptor-effector interactions are likely to participate in the control of physiological opioid effects such as tolerance and dependence.

## MATERIALS AND METHODS

### Reagents

Morphine HCl was from GlaxoSmithKline or Merck Pharma. The rabbit polyclonal phosphosite-specific antibodies anti-pS356/pT357 {4879}, anti-pT370 {3196}, anti-pS375 {2493}, anti-pT376 {3723} and anti-pT379 {3686} were generated and extensively characterized previously (10, 11, 13). The phosphorylation-independent rabbit monoclonal anti-MOP antibody {UMB-3} was obtained from Abcam-Epitomics (34). Secondary antibodies (raised in donkey) conjugated to Alexa-Fluor 488, 568 or 647 were from Jackson ImmunoResearch. Coelenterazine h was from NanoLight. Compound 101 was from HelloBio. DAMGO, ME, Calphostin C, amphotericin B and M2-anti-FLAG were from SigmaAldrich.

### Plasmids

For BRET experiments,  $\beta$ -arrestin1-YFP and  $\beta$ -arrestin2-YFP were provided by M. Caron (Duke University, NC), GRK2-Venus was from D. Jensen and Rab5a-Venus has been previously described (35). GRK2-WT and GRK2-DN (dominant negative – GRK2-K220R) were from M. Smit (Vrije Universiteit, Amsterdam). The phosphorylation deficient FLAG-MOP mutants and FLAG-MOP-RLuc8 were purchased from GeneArt. For FRET experiments, GRK2-mTurquoise and GRK2-YFP have been previously described (36).  $\beta$ -arrestin2-mTurquoise was constructed by replacing the CFP coding sequence in  $\beta$ -arrestin2-CFP (37) with mTurquoise (38). For  $\beta$ -galactosidase complementation experiments, we adapted the plasmids according to PathHunter<sup>®</sup> (DiscoverX Patent: WO 2010042921 A1, US 20100120063 A1). The plasmids were generated via artificial gene synthesis by Eurofins Genomics and cloned into pcDNA3.1. Briefly, the coding sequence for an amino-terminal HA-tag was added to the wild-type MOP and the S/T-mutant sequences, whereas the C-terminal end was fused with a Gly-rich linker (GGGGSGGGGS) and a short  $\beta$ -Gal fragment (1-

44 amino acids). All acceptor plasmids, GRKs and  $\beta$ -arrestins had the larger  $\beta$ -galactosidase synthetic sequence fragment (45-1043 amino acids) fused to their C-terminal end.

### **Small Interfering RNA Silencing of Gene Expression**

Double stranded siRNA duplexes with 3'-dTdT overhangs were obtained from Qiagen for GRK2 (5'-AAGAAAUUCAUUGAGAGCGAU-3'), GRK3 (5'-AAGCAAGCUGUAGAACACGUA-3') and a non-silencing RNA duplex (5'-GCUUAGGAGCAUUAGUAAA-3'). HEK293 cells were transfected with 150 nM siRNA for single transfection or with 100 nM of each siRNA for double transfection using HiPerFect (Qiagen). Silencing was quantified after 3 days by performing a GRK  $\beta$ -galactosidase complementation assay. All experiments showed that the siRNA reduced the target protein levels by  $\geq 80\%$ .

### **Cell Culture**

Human embryonic kidney 293 (HEK293) were maintained in Dulbecco's Modified Eagle's Medium (DMEM) supplemented with 5% v/v fetal bovine serum (FBS) at 37°C in a humidified atmosphere of 95% air and 5% CO<sub>2</sub>. Transient transfections for BRET experiments were performed using linear polyethylenimine (PEI) with a molecular weight of 25kDa (Polysciences) in a DNA:PEI ratio of 1:6 as previously described (39). For FRET experiments, transient transfections were performed in 6 cm dishes with Effectene (Qiagen) as previously described (36). For transient and stable transfections in  $\beta$ -galactosidase complementation experiments, TurboFect<sup>®</sup> DNA (Thermo Fisher Scientific) was used. Stably transfected cells were grown in medium supplemented with 400  $\mu\text{g}/\text{mL}$  G418 and/or 100  $\mu\text{g}/\text{mL}$  Hygromycin B. To increase the total number of HEK293 cells stably expressing MOP or phosphorylation-deficient mutant receptors, we used fluorescence-activated cell sorting (FACS). Trypsinized cells were washed with PBS and transferred into opti-MEM containing an A488-labeled anti-HA antibody at a dilution of 1:1000 (SigmaAldrich). After 30 min preincubation at room temperature, cells were centrifuged and the cell pellet was resuspended in

FACS buffer (2 mM EDTA, 0.5% w/v BSA in PBS). FACS was executed using a BD FACSAria III cell sorter. Approximately 1% of the positive cell population was sorted at an average purity of 85%. Sorted cells were then recultivated. To ensure similar expression levels of wild-type and mutant receptors, stable cells were characterized using Western blot analysis, surface ELISA assay and immunocytochemistry.

Patch clamp experiments were performed in AtT20 cells, which endogenously express GIRK (KirX.3) channels. Wild type MOP, <sup>354</sup>TSST<sup>357</sup>/A, <sup>375</sup>STANT<sup>379</sup>/A were all cloned in pcDNA3.0 plasmids with FLAG-tag and were expressed stably in AtT20 cells as previously described (13). For patch clamp experiments AtT20 cells were seeded on 35 mm polystyrene culture dishes (Beckton, Dickinson Biosciences) in DMEM containing 4.5 g/L glucose, penicillin-streptomycin (100µL/mL), G418 (50mg/mL) and 10% FBS (50mg/mL). Cell cultures were maintained in a humidified 5% CO<sub>2</sub> atmosphere at 37°C. Cells were ready for recording after 24 h.

### **Bioluminescence Resonance Energy Transfer (BRET)**

HEK293 cells were transiently transfected in a 10 cm dish with 1 µg of donor (RLuc8-tagged MOP wild type or phosphorylation deficient mutant) and 4 µg of acceptor (β-arrestin1-YFP, β-arrestin2-YFP, GRK2-Venus or Rab5a-Venus). For cAMP experiments cells were transiently transfected with the CAMYEL BRET biosensor (2.5 µg of FLAG-MOP and 2.5 µg of CAMYEL biosensor per dish). For GRK2 expression experiments, cells were transfected with an additional 2 µg of GRK2-WT, GRK2-DN or pcDNA3 as a control. After 24 h, cells were re-plated into poly-D-lysine-coated white opaque 96-well plates (CulturPlate, PerkinElmer) and allowed to adhere overnight. BRET experiments were performed 48 h post-transfection. Cells were washed with Hank's Balanced Salt Solution (HBSS) and equilibrated in HBSS for 30 min at 37°C prior to the experiment. Coelenterazine h was added to a final concentration of 5 µM 10 min before dual fluorescence/luminescence measurement in a LUMIstar Omega plate reader (BMG LabTech). The

BRET signal was calculated as the ratio of light emitted at 530 nm by YFP or Venus over the light emitted at 430 nm by *Renilla* luciferase 8 (RLuc8). For concentration-response curves, cells were stimulated with DAMGO ( $10^{-10}\text{M}$  –  $10^{-4}\text{M}$ ) or morphine ( $10^{-10}\text{M}$  –  $10^{-4}\text{M}$ ) for 10 min before BRET measurements. For short kinetic experiments ( $\beta$ -arrestin and GRK2 recruitment), the baseline BRET ratio was measured for 5 cycles, then either vehicle (0.01% v/v DMSO), DAMGO or morphine (both 1  $\mu\text{M}$ ) were added to the cells, and the BRET signal was measured for 30 minutes. For longer kinetic experiments (Rab5a), cells were stimulated with vehicle (0.01% v/v DMSO), DAMGO or morphine (both 1  $\mu\text{M}$ ) at different time points as stated over an interval of 100 min.

### **Förster Resonance Energy Transfer (FRET)**

To measure the interaction between MOP and  $\beta$ -arrestins, HEK293T cells were transfected with 0.8  $\mu\text{g}$  MOP-YFP (or mutants), 0.4  $\mu\text{g}$  human GRK2 and 0.8  $\mu\text{g}$   $\beta$ -Arrestin2-mTurquoise. To measure the interaction between MOP and GRK2, HEK293T cells were transfected with 0.5  $\mu\text{g}$  MOP-YFP (or mutants), 0.5  $\mu\text{g}$  rat  $\text{G}\alpha_{i1}$ , 0.5  $\mu\text{g}$  human  $\text{G}\beta_1$ , 0.4  $\mu\text{g}$  murine  $\text{G}\gamma_2$  and 0.5  $\mu\text{g}$  GRK2-mTurquoise. On the next day, cells were seeded on round 25 mm poly-lysine-coated coverslips, and 48 h post-transfection, FRET was measured as previously described (36) except that a light-emitting diode (LED) excitation system (pE-2; CoolLED) was used for all experiments. FRET traces were not corrected for bleaching effects.

### **$\beta$ -Galactosidase Complementation**

HEK293 cells stably expressing MOP or mutant MOP constructs C-terminally fused with a  $\beta$ -galactosidase enzyme fragment ( $\beta$ -Gal<sub>1-44</sub>), and stably or transiently expressing  $\beta$ -arrestins or GRKs fused to an N-terminal deletion mutant of  $\beta$ -galactosidase ( $\beta$ -Gal<sub>45-1043</sub>) were used (DiscoverX Patent: WO 2010042921 A1, US 20100120063 A1).  $\beta$ -arrestin or GRK recruitment results in complementation of the two  $\beta$ -galactosidase fragments that generate an active enzyme. Thus, levels of active enzyme are a direct result of MOP activation and are quantitated using

chemiluminescent  $\beta$ -Gal-Juice-plus<sup>®</sup> detection reagents (PJK GmbH) containing the  $\beta$ -galactoside substrate. The assay was performed as follows: cells were plated into poly-L-lysine-coated 48-well plates at a density of 125,000 cells/well in medium supplemented with 400  $\mu$ g/mL G418 and incubated overnight. After 48 h, test compounds were prepared at each concentration in DMEM and added to the cells. Following a 1 h incubation at 37°C, cell lysis reagent (1 M  $\text{NaH}_2\text{PO}_4 \cdot \text{H}_2\text{O}$ ; 1 M  $\text{Na}_2\text{HPO}_4 \cdot 2 \text{H}_2\text{O}$ , 0,1% v/v TritonX, pH 7.4) was added to each well. Luminescence was measured 1h post detection reagent addition ( $\beta$ -Gal Juice-plus<sup>®</sup>) using a FlexStation III (Molecular Devices, 500 ms integration time).

### **Western Blot**

Cells were seeded onto poly-L-lysine-coated 60 mm dishes and grown to 80 % confluence. After treatment with agonist, cells were lysed in detergent buffer (50 mM Tris-HCl, pH 7.4, 150 mM NaCl, 5 mM EDTA, 10 mM NaF, 10 mM disodium pyrophosphate, 1% v/v Nonidet P-40, 0.5% w/v sodium deoxycholate, 0.1% w/v SDS) in the presence of protease and phosphatase inhibitors (Complete mini- and PhosSTOP, Roche Diagnostics). Glycosylated proteins were partially enriched using wheat-germ lectin agarose beads as described (40, 41). Proteins were eluted from the beads using SDS-sample buffer for 20 min at 42 °C. Samples were split, resolved on 8% SDS-polyacrylamide gels, and after electroblotting membranes were incubated with either anti-pS356/pT357 {4879}, anti-pT370 {3196}, anti-pS375 {2493}, anti-pT376 {3723} or anti-pT379 {3686} antibodies followed by detection using an enhanced chemiluminescence detection system (Thermo Fisher Scientific). Blots were stripped and incubated again using the phosphorylation-independent anti-MOP antibody {UMB-3} (34) to ensure equal loading of the gels.

### **Enzyme-Linked Immunosorbent Assay (ELISA)**

HEK293 cells were transfected with 5  $\mu$ g of DNA (pcDNA3 as a control, FLAG-MOP wild type or phosphorylation deficient mutants, in 10 cm dishes), after 24 h, re-plated into poly-D-lysine coated

48-well plate and allowed to adhere overnight. After 48 h, cells were fixed with 3.7% v/v paraformaldehyde in Tris-buffered saline (TBS) for 30 min. For total expression, cells were permeabilized by 30 min incubation with 0.5% v/v NP-40 in TBS. Cells were then incubated in blocking buffer (1% w/v skim milk powder in 0.1M NaHCO<sub>3</sub>) for 4 h at room temperature and incubated with mouse M2-anti-FLAG antibody (1:2000, overnight at 4°C). After washing 3 times with TBS, cells were incubated with anti-mouse horseradish peroxidase (HRP)-conjugated antibody (1:2000) for 2 h at room temperature. Cells were washed and stained using the SIGMAFAST OPD substrate (SigmaAldrich). Absorbance at 490 nm was measured using an EnVision Multilabel Reader (PerkinElmer). Data were normalized to intact HEK293 cells transfected with MOP-WT. To measure MOP internalization, HEK293 cells stably expressing the HA-tagged MOP WT, MOP TSST-4A, MOP S375A, MOP TREHPSTANT-4A or MOP 11S/T-A were preincubated with anti-HA antibody and stimulated with 10µM DAMGO for 30 min. Receptor sequestration, quantified as the percentage of residual cell surface receptors in agonist-treated cells, was measured by ELISA as described above.

### **Confocal Imaging and Quantitative Analysis of MOP Internalization**

Stably transfected cells were grown on poly-L-lysine-coated coverslips overnight. Cells were then incubated with primary antibody (rabbit anti-HA) in serum-free medium for 2 h at 4°C. After agonist exposure, cells were fixed with 4% paraformaldehyde and 0.2% picric acid in phosphate buffer (pH 6.9) for 30 min at room temperature and washed several times with PBS. Specimens were permeabilized and then incubated with an Alexa488-conjugated goat anti-rabbit antibody (Santa Cruz Biotechnology). Specimens were mounted and examined using a Zeiss LSM510 META laser scanning confocal microscope. For quantitative internalization assays, cells were seeded onto 24-well plates. On the next day, cells were preincubated with anti-HA antibody for 2 h at 4°C. Cells

were then exposed to agonist at 37°C, fixed and developed with peroxidase-conjugated secondary antibody as described (42, 43).

## **Electrophysiology**

Patch clamp recordings were performed as previously described (13). Pipettes were pulled from borosilicate glass (AM Systems) yielding input resistances between 3.5-4.5 MΩ. For perforated patch clamp recording, pipettes were filled with internal solution containing 135 mM potassium gluconate, 3 mM MgCl<sub>2</sub>, 10 mM HEPES (adjusted to pH 7.4 with KOH). The recording electrodes were first front filled with this internal solution and then backfilled with the same solution containing 200 μg/mL amphotericin B (in 0.8% DMSO). For whole cell recording, internal solution contained 135 mM Kgluconate, 8 mM NaCl, 8 mM HEPES, 0.5 mM EGTA, 3 mM MgATP, 0.5 mM Na<sub>2</sub>GTP (pH 7.3). Cells were initially superfused with external bath solution containing 140 mM NaCl, 3 mM KCl, 1.8 mM CaCl<sub>2</sub>, 1.2 mM MgCl<sub>2</sub>, 10 mM HEPES, and 10 mM glucose (pH 7.4). For measuring I<sub>GIRK</sub>, the KCl concentration in the bath was increased to 20 mM (substituted for NaCl) before the start of the measurements and was maintained throughout the experiments as previously described in Yousuf *et al.* (2015). Liquid junction potential was calculated to be +16 mV and was adjusted before the start of each recording. Currents were recorded at 37°C in a fully enclosed, temperature-controlled recording chamber using an Axopatch 200B amplifier and pCLAMP 9.2 software, and digitized using Digidata 1320 (Axon Instruments, Molecular Devices). Currents were sampled at 100 Hz, low pass filtered at 50 Hz and recorded on hard disk for later analyses. I<sub>GIRK</sub> was recorded using a 200 ms voltage step to -120 mV from a holding potential of -60 mV delivered every 2 s. Drugs were perfused directly onto cells using a ValveLink 8.2 pressurized pinch valve perfusion system (AutoMate Scientific). In all recorded cells, solution exchange reached steady state within 200 ms (usually within 100 ms), which was confirmed by examination of the current produced at -60 mV by switching from low (3 mM) to high (20 mM) K<sup>+</sup> solution.

All data points are plotted as chord GIRK conductance ( $G_{\text{GIRK}}$ , nS) using the following calculation:  $[I_{\text{GIRK}}(-60 \text{ mV}) - I_{\text{GIRK}}(-120 \text{ mV})] \text{ pA} / 60 \text{ mV}$ . The extent of MOP desensitization as a percentage was calculated using the following formula:  $(\text{Post } G_{\text{ME}} / \text{Pre } G_{\text{ME}}) * 100$ , where, "Pre" and "Post  $G_{\text{ME}}$ " are the  $G_{\text{GIRK}}$  increase induced by a submaximal probe concentration of ME (10nM; see Supplemental Figure 6), averaged for 4-5 points during the peak response (coloured points in figures), immediately before vs 1 min after termination of exposure to a supramaximal concentration of agonist (ME 10  $\mu\text{M}$  or morphine 10  $\mu\text{M}$ ). Desensitization for different MOP mutants was analysed using a two-factor ANOVA followed by appropriate post-hoc tests as indicated.

### **Statistics**

Data are presented as the mean  $\pm$  SEM of  $n \geq 3$  independent experiments. Differences were assessed with GraphPad Prism using one-way or two-way ANOVA followed by Bonferroni adjusted post-hoc tests for multiple comparisons.

## **SUPPLEMENTARY MATERIALS**

**Supplementary Figure 1.** Expression and function of MOP phosphorylation-deficient mutants

**Supplementary Figure 2.** Inhibition of  $\beta$ -arrestin2 recruitment upon addition of naloxone

**Supplementary Figure 3.**  $\beta$ -arrestin1 recruitment and MOP internalization upon overexpression of GRK2 WT or GRK2 DN.

**Supplementary Figure 4.** GRK3 recruitment to MOP WT and mutants and inhibition of GRK2 recruitment upon addition of naloxone

**Supplementary Figure 5.** Fast desensitization component of MOP

**Supplementary Figure 6.** Patch clamp traces for corresponding MOP mutants

**Supplementary Table 1.** Potency and maximal response of MOP mutants in cAMP assay

## REFERENCES

1. J. T. Williams, S. L. Ingram, G. Henderson, C. Chavkin, M. von Zastrow, S. Schulz, T. Koch, C. J. Evans, M. J. Christie, Regulation of mu-opioid receptors: desensitization, phosphorylation, internalization, and tolerance, *Pharmacol Rev* **65**, 223–254 (2013).
2. R. A. Rudd, P. Seth, F. David, L. Scholl, Increases in drug and opioid-involved overdose deaths - United States, 2010-2015, *MMWR Morb. Mortal. Wkly. Rep.* **65**, 1445–1452 (2016).
3. H. W. Matthes, R. Maldonado, F. Simonin, O. Valverde, S. Slowe, I. Kitchen, K. Befort, A. Dierich, M. Le Meur, P. Dollé, E. Tzavara, J. Hanoune, B. P. Roques, B. L. Kieffer, Loss of morphine-induced analgesia, reward effect and withdrawal symptoms in mice lacking the mu-opioid-receptor gene, *Nature* **383**, 819–823 (1996).
4. L. M. Bohn, R. J. Lefkowitz, R. R. Gainetdinov, K. Peppel, M. G. Caron, F. T. Lin, Enhanced morphine analgesia in mice lacking beta-arrestin 2, *Science* **286**, 2495–2498 (1999).
5. K. M. Raehal, J. K. L. Walker, L. M. Bohn, Morphine side effects in beta-arrestin 2 knockout mice, *J. Pharmacol. Exp. Ther.* **314**, 1195–1201 (2005).
6. S. M. DeWire, D. S. Yamashita, D. H. Rominger, G. Liu, C. L. Cowan, T. M. Graczyk, X. T. Chen, P. M. Pitis, D. Gotchev, C. Yuan, M. Koblish, M. W. Lark, J. D. Violin, A G protein-biased ligand at the mu-opioid receptor is potently analgesic with reduced gastrointestinal and respiratory dysfunction compared with morphine, *J. Pharmacol. Exp. Ther.* **344**, 708–717 (2013).
7. A. Manglik, H. Lin, D. K. Aryal, J. D. McCorvy, D. Dengler, G. Corder, A. Levit, R. C. Kling, V. Bernat, H. Hübner, X.-P. Huang, M. F. Sassano, P. M. Giguere, S. Löber, Da Duan, G. Scherrer, B. K. Kobilka, P. Gmeiner, B. L. Roth, B. K. Shoichet, Structure-based discovery of opioid analgesics with reduced side effects, *Nature* **537**, 185–190 (2016).
8. C. L. Schmid, N. M. Kennedy, N. C. Ross, K. M. Lovell, Z. Yue, J. Morgenweck, M. D. Cameron, T. D. Bannister, L. M. Bohn, Bias factor and therapeutic window correlate to predict safer opioid analgesics, *Cell* **171**, 1165–1170.e13 (2017).
9. E. K. Lau, M. Trester-Zedlitz, J. C. Trinidad, S. J. Kotowski, A. N. Krutchinsky, A. L. Burlingame, M. von Zastrow, Quantitative encoding of the effect of a partial agonist on individual opioid receptors by multisite phosphorylation and threshold detection, *Science Signaling* **4**, ra52–ra52 (2011).
10. C. Doll, J. Konietzko, F. Pöll, T. Koch, V. Höllt, S. Schulz, Agonist-selective patterns of  $\mu$ -opioid receptor phosphorylation revealed by phosphosite-specific antibodies, *Br J Pharmacol* **164**, 298–307 (2011).
11. S. Just, S. Illing, M. Trester-Zedlitz, E. K. Lau, S. J. Kotowski, E. Miess, A. Mann, C. Doll, J. C. Trinidad, A. L. Burlingame, M. von Zastrow, S. Schulz, Differentiation of opioid drug effects by hierarchical multi-site phosphorylation, *Mol Pharmacol* **83**, 633–639 (2013).
12. V. C. Dang, B. Chieng, Y. Azriel, M. J. Christie, Cellular morphine tolerance produced by beta-arrestin-2-dependent impairment of mu-opioid receptor resensitization, *J Neurosci* **31**, 7122–7130 (2011).
13. A. Yousuf, E. Miess, S. Sianati, Y. P. Du, S. Schulz, M. Christie, The role of phosphorylation sites

in desensitization of mu-opioid receptor, *Mol Pharmacol* **88**, 825-835 (2015).

14. G. Grecksch, S. Just, C. Pierstorff, A. K. Imhof, L. Gluck, C. Doll, A. Lupp, A. Becker, T. Koch, R. Stumm, V. Holtt, S. Schulz, Analgesic tolerance to high-efficacy agonists but not to morphine is diminished in phosphorylation-deficient S375A mu-opioid receptor knock-in mice, *J Neurosci* **31**, 13890–13896 (2011).

15. D. M. Thal, R. Y. Yeow, C. Schoenau, J. Huber, J. J. G. Tesmer, molecular mechanism of selectivity among G Protein-Coupled Receptor Kinase 2 inhibitors, *Mol Pharmacol* **80**, 294–303 (2011).

16. J. D. Lowe, H. S. Sanderson, A. E. Cooke, M. Ostovar, E. Tsisanova, S. L. Withey, C. Chavkin, S. M. Husbands, E. Kelly, G. Henderson, C. P. Bailey, Role of G protein-coupled receptor kinases 2 and 3 in  $\mu$ -opioid receptor desensitization and internalization, *Mol Pharmacol* **88**, 347–356 (2015).

17. J. McPherson, G. Rivero, M. Baptist, J. Llorente, S. Al-Sabah, C. Krasel, W. L. Dewey, C. P. Bailey, E. M. Rosethorne, S. J. Charlton, G. Henderson, E. Kelly,  $\mu$ -opioid receptors: correlation of agonist efficacy for signalling with ability to activate internalization, *Mol Pharmacol* **78**, 756–766 (2010).

18. P. Molinari, V. Vezzi, M. Sbraccia, C. Gro, D. Riitano, C. Ambrosio, I. Casella, T. Costa, Morphine-like opiates selectively antagonize receptor-arrestin interactions, *J Biol Chem* **285**, 12522–12535 (2010).

19. G. L. Thompson, J. R. Lane, T. Coudrat, P. M. Sexton, A. Christopoulos, M. Canals, Biased agonism of endogenous opioid peptides at the  $\mu$ -opioid receptor, *Mol Pharmacol* **88**, 335–346 (2015).

20. J. Zhang, S. S. Ferguson, L. S. Barak, S. R. Bodduluri, S. A. Laporte, P. Y. Law, M. G. Caron, Role for G protein-coupled receptor kinase in agonist-specific regulation of mu-opioid receptor responsiveness, *Proc Natl Acad Sci U S A* **95**, 7157–7162 (1998).

21. A. Raveh, A. Cooper, L. Guy-David, E. Reuveny, Nonenzymatic rapid control of GIRK channel function by a G protein-coupled receptor kinase, *Cell* **143**, 750–760 (2010).

22. A. E. Cooke, S. Oldfield, C. Krasel, S. J. Mundell, G. Henderson, E. Kelly, Morphine-induced internalization of the L83I mutant of the rat  $\mu$ -opioid receptor, *Br J Pharmacol* **172**, 593–605 (2015).

23. W. T. Birdsong, S. Arttamangkul, J. R. Bunzow, J. T. Williams, Agonist Binding and Desensitization of the  $\mu$ -opioid receptor is modulated by phosphorylation of the C-terminal tail domain, *Mol Pharmacol* **88**, 816–824 (2015).

24. M. Connor, P. B. Osborne, M. J. Christie,  $\mu$ -Opioid receptor desensitization: Is morphine different? *Br J Pharmacol* **143**, 685–696 (2004).

25. E. A. Johnson, S. Oldfield, E. Braksator, A. Gonzalez-Cuello, D. Couch, K. J. Hall, S. J. Mundell, C. P. Bailey, E. Kelly, G. Henderson, Agonist-selective mechanisms of mu-opioid receptor desensitization in human embryonic kidney 293 cells, *Mol Pharmacol* **70**, 676–685 (2006).

26. M. L. Halls, H. R. Yeatman, C. J. Nowell, G. L. Thompson, A. B. Gondin, S. Civciristov, N. W. Bunnett, N. A. Lambert, D. P. Poole, M. Canals, Plasma membrane localization of the  $\mu$ -opioid receptor controls spatiotemporal signaling, *Science Signaling* **9**, ra16 (2016).

27. L. Glück, A. Loktev, L. Moulédous, C. Mollereau, P.-Y. Law, S. Schulz, Loss of morphine reward and dependence in mice lacking G protein-coupled receptor kinase 5, *Biol Psychiatry*, 1–8 (2014).
28. H. Haberstock-Debic, M. Wein, M. Barrot, E. E. O. Colago, Z. Rahman, R. L. Neve, V. M. Pickel, E. J. Nestler, M. von Zastrow, A. L. Svingos, Morphine acutely regulates opioid receptor trafficking selectively in dendrites of nucleus accumbens neurons, *J Neurosci* **23**, 4324–4332 (2003).
29. J. A. Trafton, C. Abbadie, K. Marek, A. I. Basbaum, Postsynaptic signaling via the [mu]-opioid receptor: responses of dorsal horn neurons to exogenous opioids and noxious stimulation, *J Neurosci* **20**, 8578–8584 (2000).
30. D. Zindel, S. Engel, A. R. Bottrill, J.-P. Pin, L. Prezeau, A. B. Tobin, M. Bünemann, C. Krasel, A. J. Butcher, Identification of key phosphorylation sites in PTH1R that determine arrestin3 binding and fine-tune receptor signaling, *Biochem J* **473**, 4173–4192 (2016).
31. L. E. Gimenez, S. Kook, S. A. Vishnivetskiy, M. R. Ahmed, E. V. Gurevich, V. V. Gurevich, Role of Receptor-attached Phosphates in Binding of Visual and Non-visual Arrestins to G Protein-coupled Receptors, *J Biol Chem* **287**, 9028–9040 (2012).
32. S. Illing, A. Mann, S. Schulz, Heterologous regulation of agonist-independent  $\mu$ -opioid receptor phosphorylation by protein kinase C, *Br J Pharmacol* **171**, 1330–1340 (2014).
33. A. Mann, S. Illing, E. Miess, S. Schulz, Different mechanisms of homologous and heterologous  $\mu$ -opioid receptor phosphorylation, *Br J Pharmacol* **172**, 311–316 (2015).
34. A. Lupp, N. Richter, C. Doll, F. Nagel, S. Schulz, Regulatory Peptides, *Regulatory Peptides* **167**, 9–13 (2011).
35. T.-H. Lan, Q. Liu, C. Li, G. Wu, N. A. Lambert, Sensitive and high resolution localization and tracking of membrane proteins in live cells with BRET, *Traffic (Copenhagen, Denmark)* **13**, 1450–1456 (2012).
36. V. Wolters, C. Krasel, J. Brockmann, M. Bünemann, Influence of G q on the dynamics of M3-acetylcholine receptor-G-protein-coupled receptor kinase 2 interaction, *Mol Pharmacol* **87**, 9–17 (2015).
37. C. Krasel, M. Bünemann, K. Lorenz, M. J. Lohse, beta-Arrestin binding to the beta2-adrenergic receptor requires both receptor phosphorylation and receptor activation, *J Biol Chem* **280**, 9528–9535 (2005).
38. J. Goedhart, L. van Weeren, M. A. Hink, N. O. E. Vischer, K. Jalink, T. W. J. Gadella, Bright cyan fluorescent protein variants identified by fluorescence lifetime screening, *Nat Meth* **7**, 137–139 (2010).
39. M. L. Halls, D. P. Poole, A. M. Ellisdon, C. J. Nowell, M. Canals, in *Methods in Molecular Biology*, Methods in Molecular Biology. (Springer New York, New York, NY, 2015), vol. 1335, pp. 131–161.
40. S. Schulz, D. Mayer, M. Pfeiffer, R. Stumm, T. Koch, V. Höllt, Morphine induces terminal micro-opioid receptor desensitization by sustained phosphorylation of serine-375, *The EMBO Journal* **23**, 3282–3289 (2004).
41. T. Koch, C-terminal splice variants of the mouse micro-opioid receptor differ in morphine-

induced internalization and receptor resensitization, *J Biol Chem* **276**, 31408–31414 (2001).

42. S. Lesche, D. Lehmann, F. Nagel, H. A. Schmid, S. Schulz, Differential effects of octreotide and pasireotide on somatostatin receptor internalization and trafficking in vitro, *J Clin Endocrinol Metab* **94**, 654–661 (2009).

43. F. Poll, C. Doll, S. Schulz, Rapid dephosphorylation of G protein-coupled receptors by protein phosphatase 1 is required for termination of beta-arrestin-dependent signaling, *J Biol Chem* **286**, 32931–32936 (2011).

## NOTES

**Acknowledgments:** The authors thank Dr. A. Stewart for technical assistance.

**Funding:** This work was supported by a Deutsche Forschungsgemeinschaft Grant SFB/TR166-TPC5 to S.S.; a Monash Fellowship to M.C.; National Health and Medical Research Council (NHMRC) RD Wright Fellowship to M.L.H. (1061687) and an NHMRC Project Grant 1121029 to M.C. and M.L.H.

**Author contributions:** E.M. performed and analyzed the data of  $\beta$ -Gal experiments; A.B.G performed and analyzed the data of BRET experiments; A.Y. performed and analyzed electrophysiology experiments; R.S performed and analyzed the data of some  $\beta$ -Gal experiments; N.M., Y.Y. and M.G. performed and analyzed the data FRET experiments; J.G.R. generated FRET constructs/reagents; M.B. and C.K. supervised FRET experiments; M.J.C. supervised electrophysiology experiments; M.L.H. and M.C. supervised BRET experiments; S.S. supervised  $\beta$ -Gal experiments. E.M., A.B.G and M.C wrote manuscript. All authors reviewed the manuscript.

**Competing interests:** The authors declare that they have no competing interests.

## FIGURES

**Figure 1. Agonist-dependent recruitment of  $\beta$ -arrestin1 and 2 to wild-type MOP.** (A) Schematic representation of the approaches used in this study: BRET, FRET and  $\beta$ -galactosidase complementation. (B) HEK293 cells expressing MOP-RLuc8 and  $\beta$ -arrestin2-YFP (BRET) were stimulated with 1  $\mu$ M DAMGO or morphine for 20 min prior to addition of 30  $\mu$ M naloxone (n=4). (C) HEK293 cells expressing MOP-YFP and  $\beta$ -arrestin2-CFP (FRET) were stimulated with 10 $\mu$ M DAMGO or 30 $\mu$ M morphine for 1 min prior to agonist washout (n=6). (D, E) HEK293 cells expressing MOP-RLuc8 and  $\beta$ -arrestin1/2-YFP (BRET) were stimulated for 10 min with increasing concentrations of DAMGO or morphine (n=6). (F, G) HEK293 cells expressing MOP- $\beta$ -Gal1-44 and  $\beta$ -arrestin1/2- $\beta$ -Gal45-1043 ( $\beta$ -Gal complementation) were stimulated with increasing concentrations of DAMGO or morphine for 1 h (n=4-6). Raw BRET/FRET ratio of vehicle-treated cells was subtracted and raw bioluminescence data from  $\beta$ -gal were normalized to vehicle-treated cells. Data points represent mean $\pm$ SEM of the indicated number of experiments.

**Figure 2. C-tail phosphorylation of MOP.** (A) Schematic representation of the C-tail domain of mouse MOP with potential phosphate acceptor sites depicted in grey and phosphosite-specific antibodies against pS/pT residues depicted in black (pS356/pT357, pT370, pS375, pT376 and pT379). The epitope recognized by the phospho-independent antibody UMB-3 is underlined. (B) C-tail sequences of wild-type MOP (WT) and phosphorylation-deficient MOP mutants are also illustrated. Serine (S) and threonine (T) residues depicted in black were mutated to alanine (A) depicted in grey as shown in each of the mutants. (C) Characterization of phosphosite-specific antibodies using Western blot analysis. HEK293 cells stably expressing the HA-tagged MOP WT, MOP TSST-4A, MOP S375A, MOP TREHPSTANT-4A or MOP 11S/T-A, were stimulated with 10 $\mu$ M DAMGO or morphine for 30 min at 37°C. Cells were lysed and immunoblotted with anti-pS356/pT357, anti-pT370, anti-pS375, anti-pT376 or anti-pT379 antibodies. Blots were stripped

and reprobed with the phosphorylation-independent anti-MOP antibody UMB-3 or with anti-HA antibody to confirm equal loading.

**Figure 3. Recruitment of  $\beta$ -arrestin1 and 2 to phosphorylation-deficient MOP mutants. (A, B)** (A) HEK293 cells were transiently transfected with MOP-RLuc8 WT or phosphorylation-deficient mutants and  $\beta$ -arrestin1/2-YFP (BRET) and stimulated for 30min with 1 $\mu$ M DAMGO or morphine (n=3-5). Raw BRET ratio of vehicle-treated cells was subtracted and data represent mean $\pm$ SEM. Area under the curve (AUC) of BRET signal is shown as a percentage of the maximal response to DAMGO in the WT receptor and represents means $\pm$ SEM. All responses are significant against vehicle; ^ denotes significance vs WT (p<0.01) two-way ANOVA with Dunnett's multiple comparison test; \* denotes significance of DAMGO vs morphine (p<0.01) two-way ANOVA with Sidak's multiple comparison test. (B) HEK293 cells expressing MOP-RLuc8 WT or phosphorylation-deficient mutants and  $\beta$ -arrestin2-YFP (BRET) or MOP- $\beta$ -Gal1-44 WT or phosphorylation-deficient mutants and  $\beta$ -arrestin2- $\beta$ -Gal45-1043 ( $\beta$ -Gal complementation) were stimulated with increasing concentrations of DAMGO or morphine for 10 min or 1 h, respectively. Data were normalized to vehicle-treated cells and represent mean $\pm$ SEM (n=3-6). (C) HEK293 cells expressing MOP-RLuc8 WT or phosphorylation-deficient mutants and  $\beta$ -arrestin1-YFP (BRET) or MOP- $\beta$ -Gal1-44 WT or phosphorylation-deficient mutants and  $\beta$ -arrestin1- $\beta$ -Gal45-1043 ( $\beta$ -Gal complementation) were stimulated with increasing concentrations of DAMGO or morphine for 10 min or 1 h, respectively. Data were normalized to vehicle-treated cells and represent mean $\pm$ SEM (n=3-6). (D) HEK293 cells expressing MOP-YFP phosphorylation-deficient mutants and  $\beta$ -arrestin2-CFP (FRET) were stimulated with 10 $\mu$ M DAMGO or 30 $\mu$ M morphine for 1min prior to agonist washout (left panel n=14 for WT and n=15 for S375A; right panel n=17 for WT and 11S/T-A). n, number of experiments

**Figure 4. Internalization of phosphorylation-deficient MOP mutants. (A)** Internalization BRET assay in HEK293 cells transiently transfected with MOP-RLuc8 WT or phosphorylation-deficient

mutants and the early endosome marker Rab5a-Venus and stimulated with 1 $\mu$ M DAMGO. BRET ratio of vehicle-treated cells was subtracted. Data points represent mean $\pm$ SEM (n=3-4). (B) HEK293 cells stably expressing the HA-tagged MOP WT, MOP TSST-4A, MOP S375A, MOP TREHPSTANT-4A or MOP 11S/T-A were preincubated with anti-HA antibody and stimulated with 10 $\mu$ M DAMGO for 30 min. Receptor sequestration, quantified as the percentage of residual cell surface receptors on agonist-treated cells, was measured by ELISA (n=3). n, number of experiments

**Figure 5. Role of GRKs in  $\beta$ -arrestin recruitment.** (A, B) HEK293 cells expressing MOP-RLuc8 and  $\beta$ -arrestin2-YFP (BRET) and pcDNA3 (mock), GRK2-WT or GRK2-DN were stimulated for 10min with increasing concentrations of DAMGO or morphine and the BRET signal measured after stimulation (n=3). (C, D) HEK293 cells expressing MOP- $\beta$ -Gal1-44 and  $\beta$ -arrestin1/2- $\beta$ -Gal45-1043 ( $\beta$ -Gal complementation) and mock (pcDNA3), GRK2 or GRK3 for overexpression were stimulated with increasing concentrations of DAMGO or morphine for 1 h (n=3-6). For BRET, the ratio of vehicle-treated cells was subtracted and for  $\beta$ -Gal, the data were normalized to vehicle-treated cells. Data points represent mean $\pm$ SEM. (E) HEK293 cells expressing MOP alone (control) or in combination with pcDNA3 (mock), GRK2, GRK3 or both were stimulated with 10 $\mu$ M morphine for 30 min at 37°C, lysed and immunoblotted with anti-pT370, anti-pS375, or anti-pT379 antibodies. Blots were stripped and reprobed with the phosphorylation-independent anti-HA antibody to confirm equal loading. (F) HEK293 cells expressing MOP- $\beta$ -Gal1-44 and  $\beta$ -arrestin1/2- $\beta$ -Gal45-1043 ( $\beta$ -Gal complementation) were co-transfected with scrambled (SCR), GRK2 or GRK3 siRNA and stimulated with increasing concentrations of DAMGO or morphine for 1 h (n=4). Raw BRET ratio of vehicle-treated cells was subtracted and raw bioluminescence data from  $\beta$ -Gal were normalized to vehicle-treated cells. (G) HEK293 cells expressing MOP-RLuc8 and  $\beta$ -arrestin2-YFP (BRET) were incubated in a control or 30  $\mu$ M Cmpd101 pretreatment condition for 30 min prior stimulation with 1 $\mu$ M DAMGO or morphine (n=4). Area under the curve (AUC) is expressed as a percentage of

the maximal response of DAMGO in the control and is shown as the mean±SEM. ^ denotes significance vs control ( $p<0.01$ ), two-way ANOVA with Dunnett's multiple comparison test. n, number of experiments

**Figure 6. GRK recruitment to activated wild-type MOP.** (A) HEK293 cells expressing MOP-YFP and GRK2-mTurquoise (FRET) were stimulated with 10  $\mu$ M DAMGO or 30  $\mu$ M morphine for 1 min prior to agonist washout (n=6). (B, C) HEK293 cells expressing MOP-RLuc8 and GRK2-Venus (BRET) were stimulated with 1  $\mu$ M DAMGO or morphine for 20 min prior further addition of 30  $\mu$ M naloxone (B) or for 10 min with increasing concentrations of DAMGO and morphine (C) (both n=3). (D) HEK293 cells expressing MOP- $\beta$ -Gal1-44 and GRK2- $\beta$ -Gal45-1043 ( $\beta$ -Gal complementation) were stimulated with increasing concentrations of DAMGO or morphine for 1 h (n=4). For BRET/FRET, data from vehicle-treated cells was subtracted, and for  $\beta$ -Gal the data were normalized to vehicle-treated cells. Data represent mean±SEM. (E) HEK293 cells expressing MOP-RLuc8 and GRK2-Venus (BRET) were incubated with control or 30  $\mu$ M Cmpd101 for 30 min prior to stimulation with 1  $\mu$ M DAMGO or morphine. The 10 min area under the curve (AUC) was quantified and is expressed as a percentage of the maximal response of the control-treated DAMGO response (n=4). Data are expressed as mean±SEM. ^ denotes significance vs control ( $p<0.01$ ) in two-way ANOVA with Dunnett's multiple comparison test. n, number of experiments

**Figure 7. GRK2 recruitment to phosphorylation-deficient MOP mutants.** (A, B) HEK293 cells were transiently transfected with MOP-RLuc8 WT or phosphorylation-deficient mutants and GRK2-Venus (BRET) and stimulated for 30 min with 1  $\mu$ M DAMGO (A) or for 10 min with increasing concentrations of DAMGO or morphine (B) (both n=3). The BRET ratio of vehicle-treated cells was subtracted and data represent mean±SEM. The area under the curve (AUC) is expressed as a percentage of the maximal response to DAMGO by the WT receptor and represents mean±SEM. All responses are significant vs vehicle; ^ denotes significance vs WT ( $p<0.01$ ), two-way ANOVA

with Dunnett's multiple comparison test; \* denotes significance of DAMGO vs morphine ( $p < 0.01$ ), two-way ANOVA with Sidak's multiple comparison test. **(C)** HEK293 cells expressing MOP- $\beta$ -Gal1-44 WT or phosphorylation-deficient mutants and GRK2- $\beta$ -Gal45-1043 ( $\beta$ -Gal complementation) were stimulated with increasing concentrations of DAMGO for 1 h ( $n=3-4$ ). Data were normalized to vehicle-treated cells, and represent the mean  $\pm$  SEM. **(D)** HEK293 cells expressing MOP-YFP phosphorylation-deficient mutants and GRK2-mTurquoise (FRET) were stimulated with 10  $\mu$ M DAMGO or 30  $\mu$ M morphine for 1 min prior to agonist washout (left panel  $n=14$  for WT and  $n=17$  for S375A; right panel  $n=14$  for WT and  $n=13$  for 11S/T-A).  $n$ , number of experiments

**Figure 8. Acute desensitization in perforated patch clamp vs whole cell patch clamp recording mode by different MOP mutants.** Extent of desensitization was determined by exposure to a submaximal concentration of ME (M; 10nM, in red), as described in the text, before and after exposure to supramaximal concentrations of ME (10 $\mu$ M, orange) as shown in traces A, B and C. **(A)** Exemplar records of MOP-mediated  $G_{GIRK}$  for ME-induced desensitization in WT and STANT-3A mutant. **(B)** Exemplar records showing loss of ME induced desensitization only in the STANT-3A mutant using whole cell patch clamp and, alternatively **(C)**, in perforated patch clamp mode after pre-treatment with 30nM Calphostin-C. **(D)**, **(E)** and **(F)** compare acute desensitization using whole cell and perforated patch clamp recordings in different mutants ( $n=5$  for each cell type). All scale bars represent 0.2 nS and 1 min. Two-way ANOVAs for **(D)**, **(E)** and **(F)** were all significant for main effects. Post hoc comparisons (Bonferroni corrected) were significant where shown (\*\*\*\*  $P < 0.0001$ ). In **(D)** post- compared with pre-desensitized response [100 %]; the main effect of ME vs morphine was not significant ( $P > 0.05$ ).

## TABLES

**Table 1. Potency (pEC<sub>50</sub>) and maximal response (E<sub>max</sub>) of β-arrestin1 and 2 recruitment to wild-type MOP by BRET and β-Gal complementation.**

MOP WT		BRET		β-Gal	
		pEC <sub>50</sub> (EC <sub>50</sub> μM)	E <sub>max</sub> (% of DAMGO)	pEC <sub>50</sub> (EC <sub>50</sub> μM)	E <sub>max</sub> (% of DAMGO)
β-arrestin1	DAMGO	6.05 ± 0.06 (0.89)	100	5.82 ± 0.07 (1.51)	100
	Morphine	-	-	-	-
β-arrestin2	DAMGO	6.28 ± 0.04 (0.52)	100	5.94 ± 0.03 (1.15)	100
	Morphine	6.12 ± 0.05 (0.76)	33.57 ± 2.18	6.00 ± 0.05 (1.00)	39.91 ± 1.01

**Table 2. Potency (pEC<sub>50</sub>) and maximal response (E<sub>max</sub>) of β-arrestin1 recruitment to phosphorylation-deficient MOP mutants.**

MOP		BRET		β-Gal	
		pEC <sub>50</sub>	E <sub>max</sub> (% of WT DAMGO)	pEC <sub>50</sub>	E <sub>max</sub> (% of WT DAMGO)
WT	DAMGO	6.05 ± 0.06	100	5.82 ± 0.07	100
	Morphine	-	-	-	-
TSST-4A	DAMGO	6.10 ± 0.06	91.59 ± 1.56	5.86 ± 0.05	36.33 ± 6.79
	Morphine	-	-	-	-
S375A	DAMGO	5.89 ± 0.07	36.20 ± 6.27 <sup>^</sup>	6.71 ± 0.13	32.20 ± 5.73
	Morphine	-	-	-	-
TREPSTANT-4A	DAMGO	-	-	5.95 ± 0.48	28.47 ± 7.18
	Morphine	-	-	-	-
11S/T-A	DAMGO	-	-	8.27 ± 1.74	23.46 ± 2.33
	Morphine	-	-	-	-

<sup>^</sup> denotes significance vs WT (p<0.01) two-way ANOVA with Dunnett's multiple comparison test.

**Table 3. Potency (pEC<sub>50</sub>) and maximal response (E<sub>max</sub>) of β-arrestin2 recruitment to phosphorylation-deficient MOP mutants.**

MOP		BRET		$\beta$ -Gal	
		pEC <sub>50</sub>	E <sub>max</sub> (% of WT DAMGO)	pEC <sub>50</sub>	E <sub>max</sub> (% of WT DAMGO)
WT	DAMGO	6.28 ± 0.04	100	5.94 ± 0.03	100
	Morphine	6.12 ± 0.05	33.57 ± 2.18	-	-
TSST-4A	DAMGO	6.36 ± 0.02	94.08 ± 3.76	5.58 ± 0.05	56.73 ± 7.61
	Morphine	5.85 ± 0.14	29.21 ± 4.11	-	-
S375A	DAMGO	6.30 ± 0.01	71.73 ± 6.47 <sup>^</sup>	6.08 ± 0.18	49.36 ± 16.95
	Morphine	6.37 ± 0.14	17.31 ± 0.90 <sup>^</sup>	-	-
STANT-3A	DAMGO	6.20 ± 0.06	56.26 ± 1.81 <sup>^</sup>	NA	NA
	Morphine	6.40 ± 0.08	14.76 ± 1.66 <sup>^</sup>	NA	NA
TREPSTANT-4A	DAMGO	NA	NA	5.72 ± 0.05	42.55 ± 6.31
	Morphine	NA	NA	-	-
11S/T-A	DAMGO	6.16 ± 0.02	41.90 ± 5.48 <sup>^</sup>	6.08 ± 0.17	43.73 ± 5.16
	Morphine	6.29 ± 0.08	15.92 ± 1.67 <sup>^</sup>	-	-

<sup>^</sup> denotes significance vs WT (p<0.01) two-way ANOVA with Dunnett's multiple comparison test.

**Table 4. Potency (pEC<sub>50</sub>) and maximal response (E<sub>max</sub>) of  $\beta$ -arrestin2 recruitment with GRK overexpression (OE) or knockdown (KD).**

MOP		BRET		$\beta$ -Gal	
		pEC <sub>50</sub>	E <sub>max</sub> (% of mock DAMGO)	pEC <sub>50</sub>	E <sub>max</sub> (% of mock or SRC)
Mock	DAMGO	6.50 ± 0.02	100	5.72 ± 0.02	100
	Morphine	5.95 ± 0.05	25.72 ± 2.10	6.51 ± 0.38	100
GRK2-WT OE	DAMGO	8.03 ± 0.04 <sup>^</sup>	176.43 ± 8.43 <sup>^</sup>	5.81 ± 0.01	128.98 ± 17.03
	Morphine	7.33 ± 0.05 <sup>^</sup>	146.06 ± 6.18 <sup>^</sup>	6.16 ± 0.26	183.99 ± 28.26
GRK2-DN OE	DAMGO	6.41 ± 0.03	62.23 ± 3.18 <sup>^</sup>	-	-
	Morphine	6.55 ± 0.02	12.56 ± 1.66	-	-
GRK3-WT OE	DAMGO	NA	NA	6.51 ± 0.03	157.94 ± 18.66
	Morphine	NA	NA	6.05 ± 0.14	144.58 ± 40.65
SCR	DAMGO	NA	NA	5.71 ± 0.13	100
	Morphine	NA	NA	-	-
GRK2 KD	DAMGO	NA	NA	6.09 ± 0.12	72.39 ± 4.35
	Morphine	NA	NA	-	-
GRK3 KD	DAMGO	NA	NA	6.14 ± 0.15	85.64 ± 2.51
	Morphine	NA	NA	-	-

<sup>^</sup> denotes significance vs WT (p<0.01) two-way ANOVA with Dunnett's multiple comparison test.

**Table 5. Potency (pEC<sub>50</sub>) and maximal response (E<sub>max</sub>) of GRK2 recruitment to wild type MOP by BRET and  $\beta$ -Gal complementation.**

MOP WT	BRET		$\beta$ -Gal	
	pEC <sub>50</sub>	E <sub>max</sub>	pEC <sub>50</sub>	E <sub>max</sub>

		(EC <sub>50</sub> μM)	(% of DAMGO)	(EC <sub>50</sub> μM)	(% of DAMGO)
<b>GRK2</b>	<b>DAMGO</b>	6.22 ± 0.14 (0.6)	100	6.39 ± 0.12 (0.41)	100
	<b>Morphine</b>	6.37 ± 0.20 (0.43)	37.88 ± 7.22	6.57 ± 0.36 (0.27)	56.13 ± 9.64

**Table 6. Potency (pEC<sub>50</sub>) and maximal response (E<sub>max</sub>) of GRK2 recruitment to phosphorylation-deficient MOP mutants.**

<b>MOP</b>		<b>BRET</b>		<b>β-Gal</b>	
		pEC <sub>50</sub>	E <sub>max</sub> (% of WT DAMGO)	pEC <sub>50</sub>	E <sub>max</sub> (% of WT DAMGO)
<b>WT</b>	<b>DAMGO</b>	6.22 ± 0.14	100	6.39 ± 0.12	100
	<b>Morphine</b>	6.37 ± 0.20	37.88 ± 7.22	-	-
<b>TSST-4A</b>	<b>DAMGO</b>	6.50 ± 0.13	99.02 ± 9.38	5.72 ± 0.11	45.35 ± 1.58 <sup>^</sup>
	<b>Morphine</b>	6.47 ± 0.08	42.72 ± 11.93	-	-
<b>S375A</b>	<b>DAMGO</b>	6.08 ± 0.05	86.02 ± 3.79	5.80 ± 0.09	40.15 ± 7.32 <sup>^</sup>
	<b>Morphine</b>	5.92 ± 0.27	30.36 ± 7.33	-	-
<b>STANT-3A / TREHPSTANT- 4A</b>	<b>DAMGO</b>	5.77 ± 0.15	58.33 ± 6.62 <sup>^</sup>	6.15 ± 0.38	36.73 ± 4.27 <sup>^</sup>
	<b>Morphine</b>	5.63 ± 0.51	26.77 ± 5.45	-	-
<b>11S/T-A</b>	<b>DAMGO</b>	5.77 ± 0.08	53.33 ± 2.48 <sup>^</sup>	6.13 ± 1.46	33.86 ± 3.64 <sup>^</sup>
	<b>Morphine</b>	5.57 ± 0.05	23.20 ± 3.11	-	-

<sup>^</sup> denotes significance vs WT (p<0.01) two-way ANOVA with Dunnett's multiple comparison test.

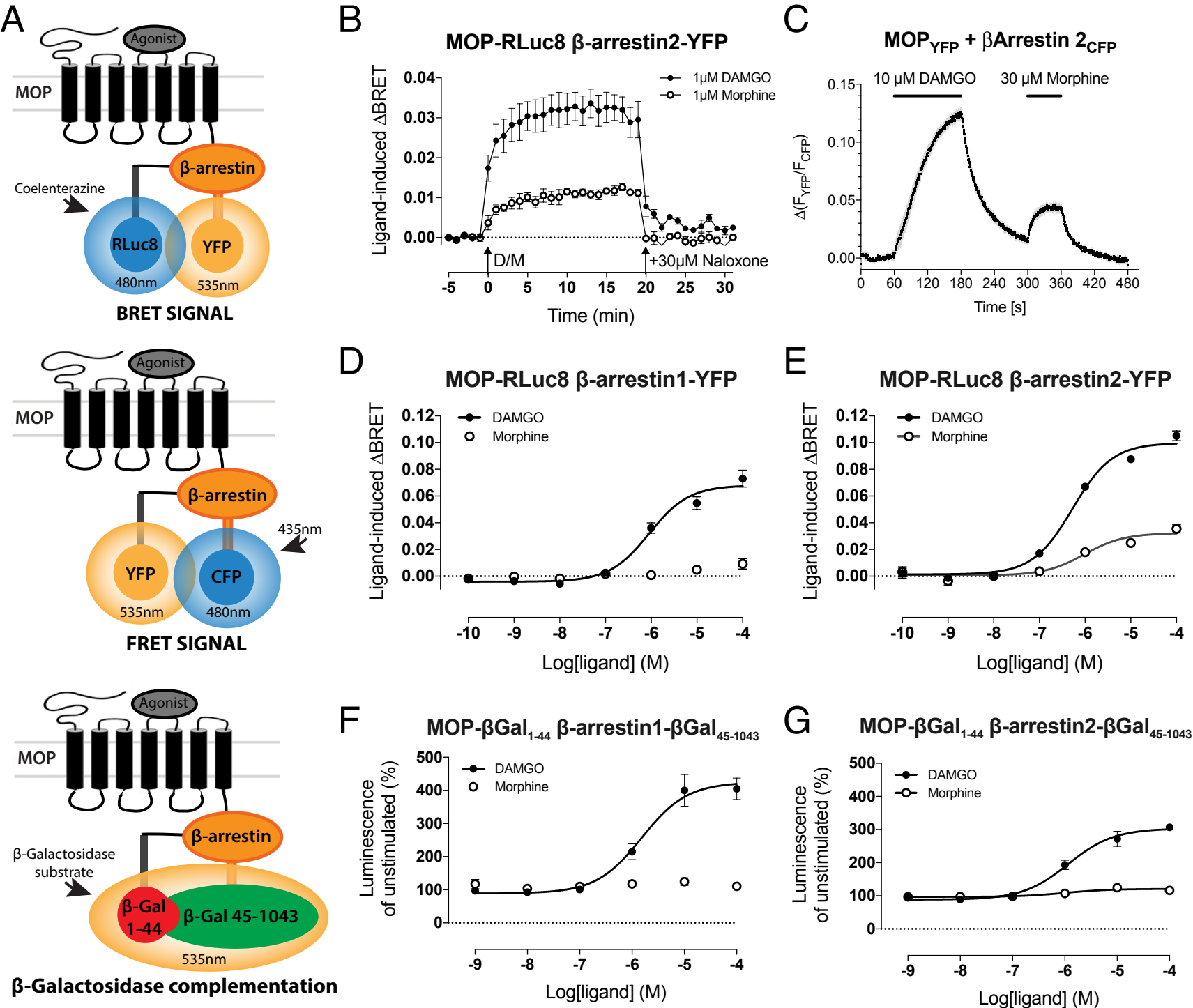
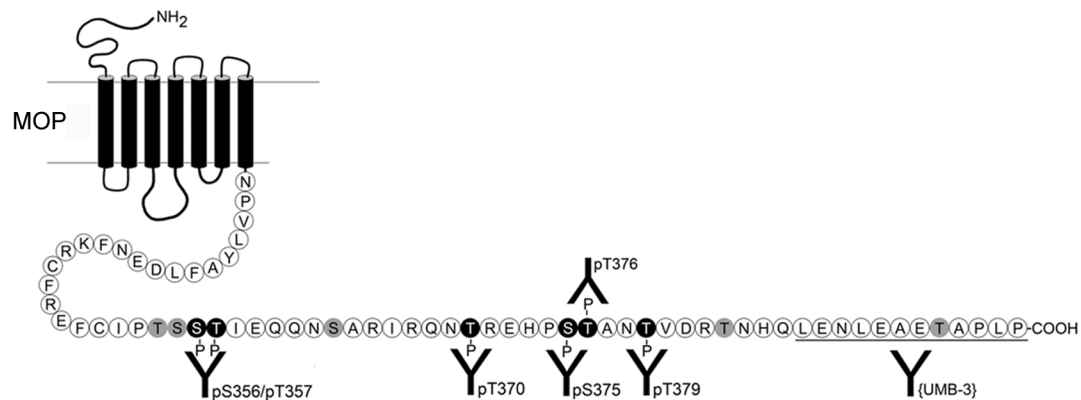
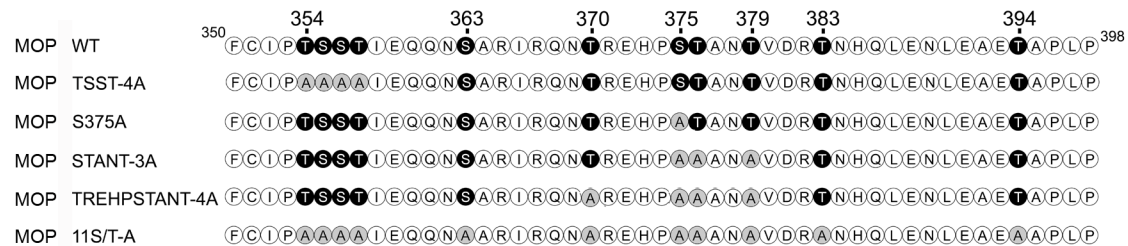


**Figure 1**

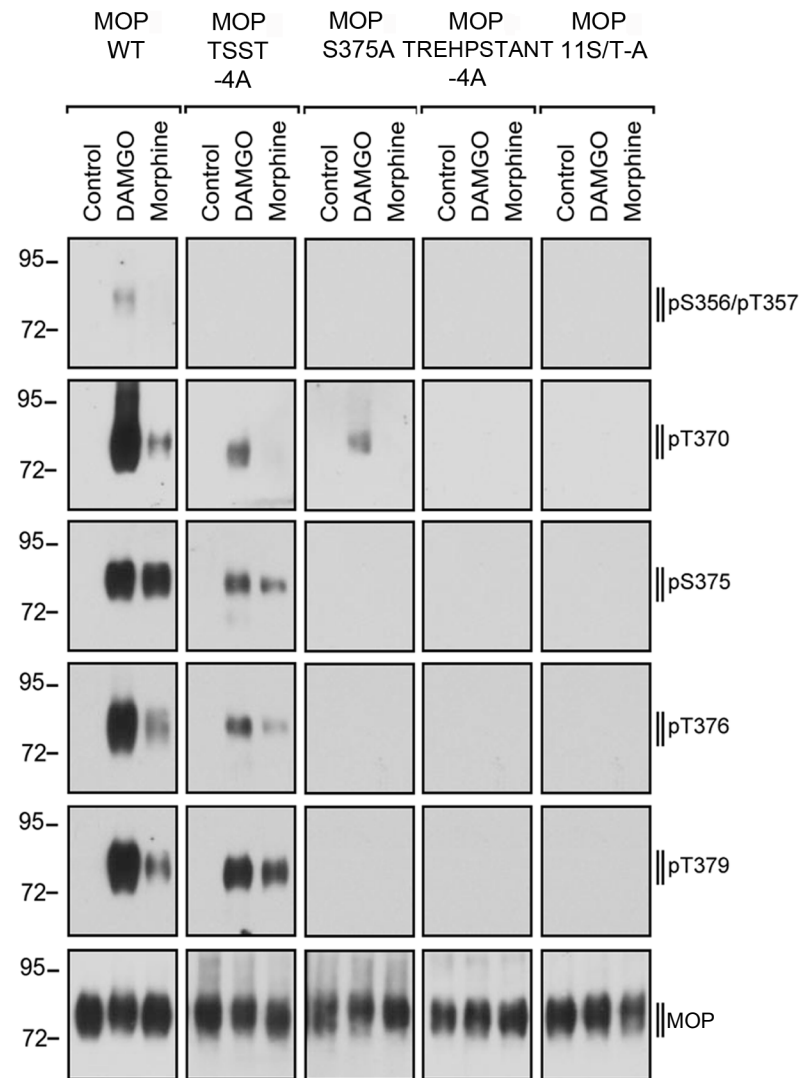
A

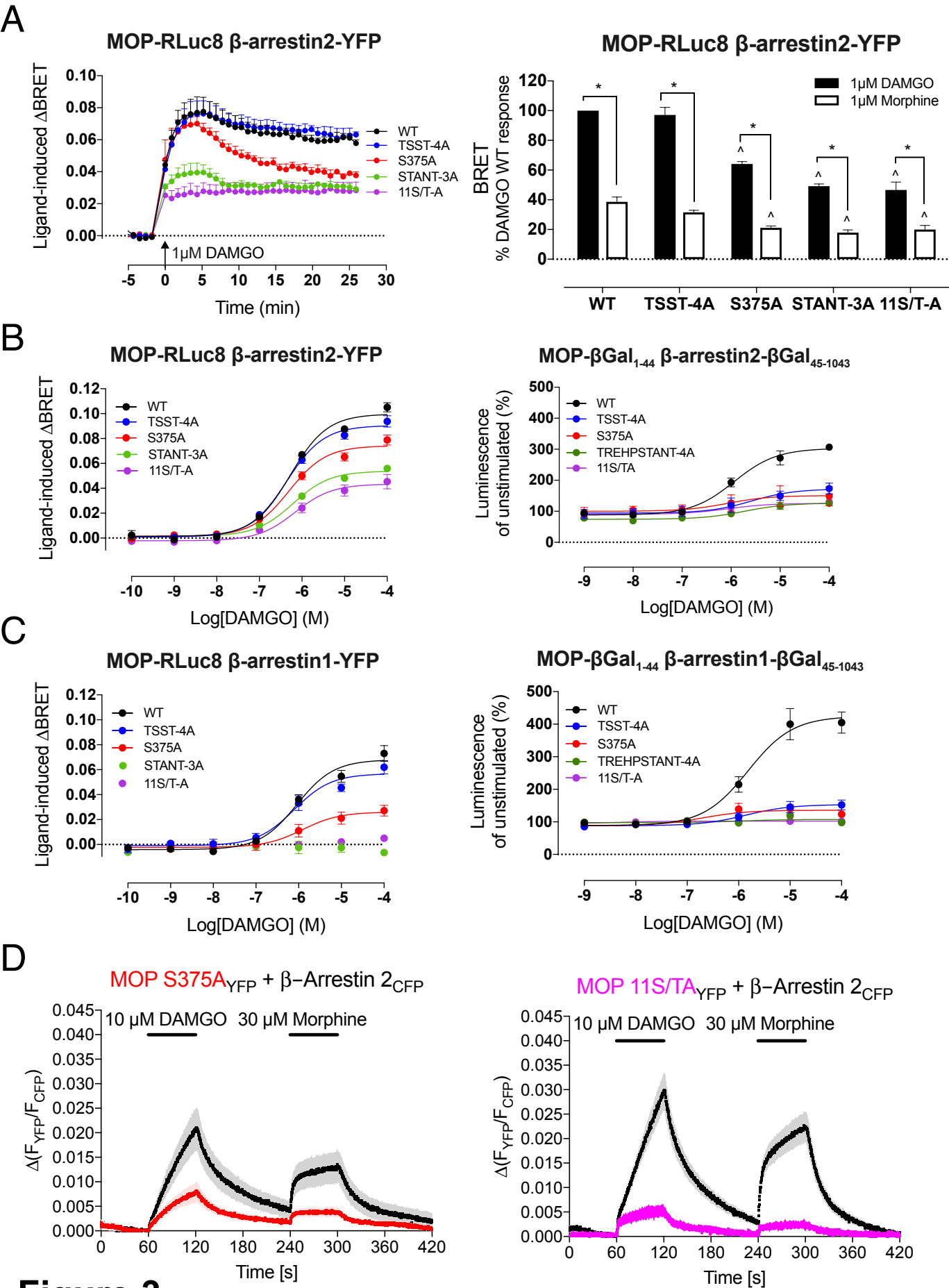


B

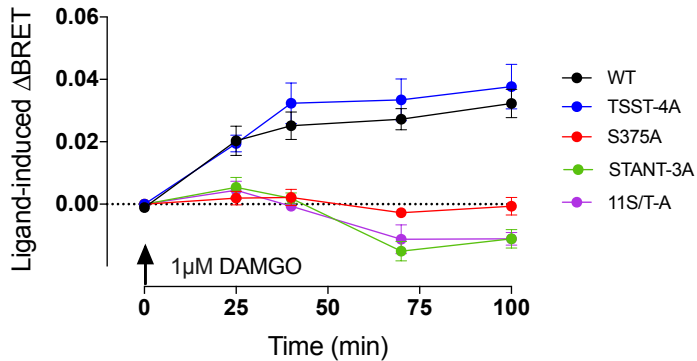
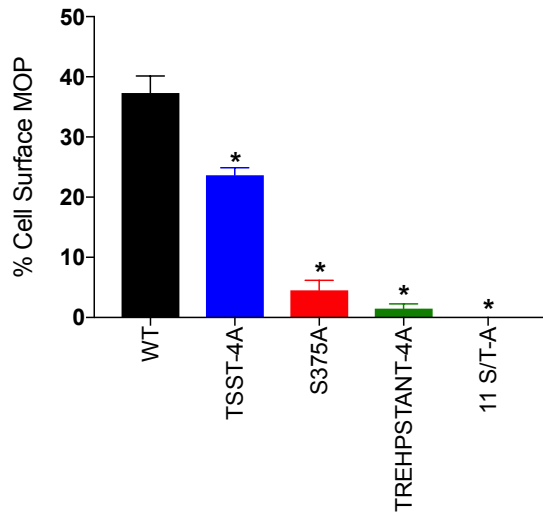


C





**Figure 3**

**A****MOP-RLuc8 Rab5a-Venus****B****Figure 4**

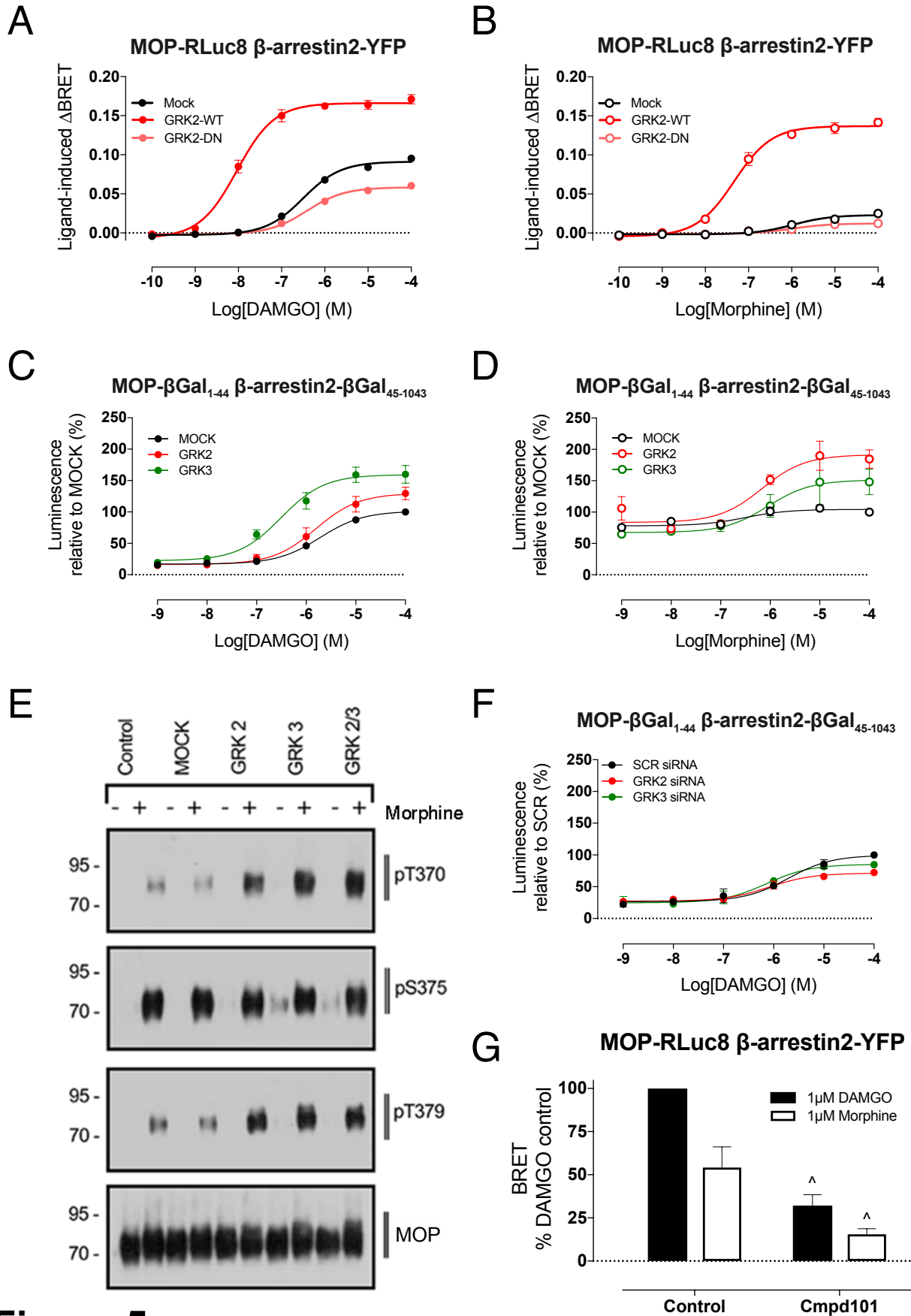


**Figure 5**

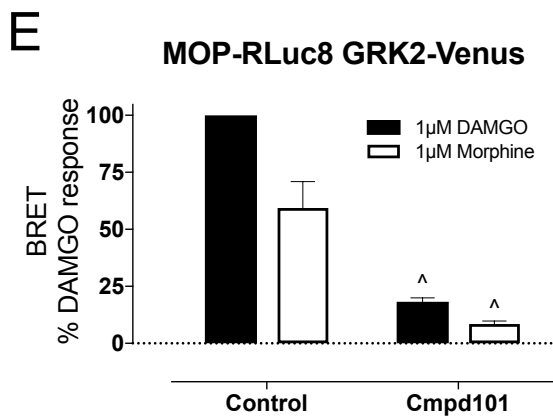
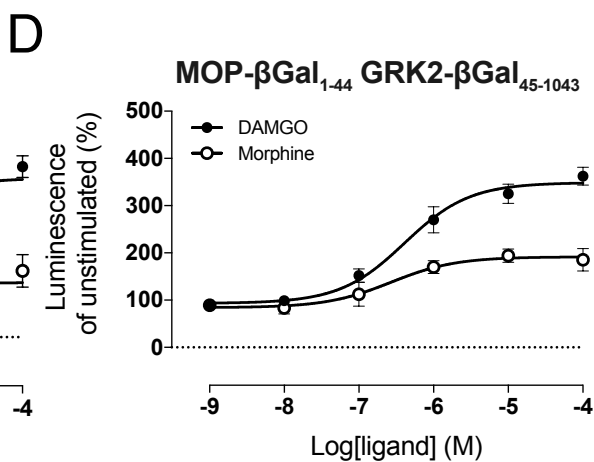
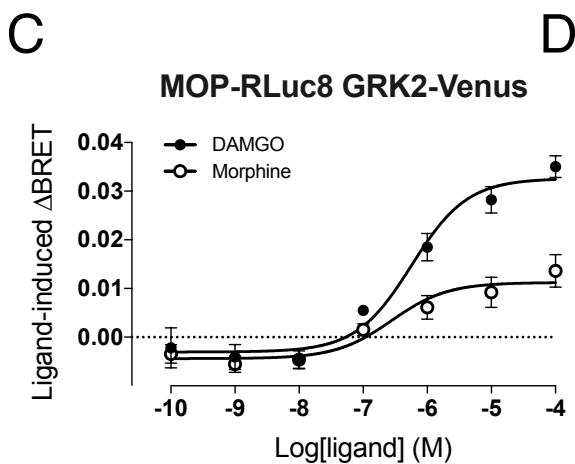
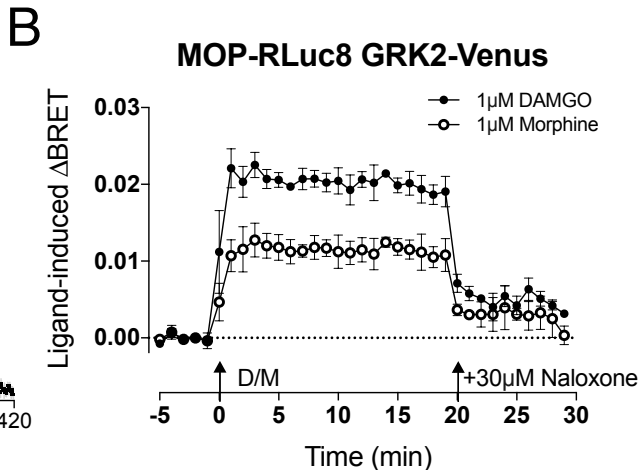
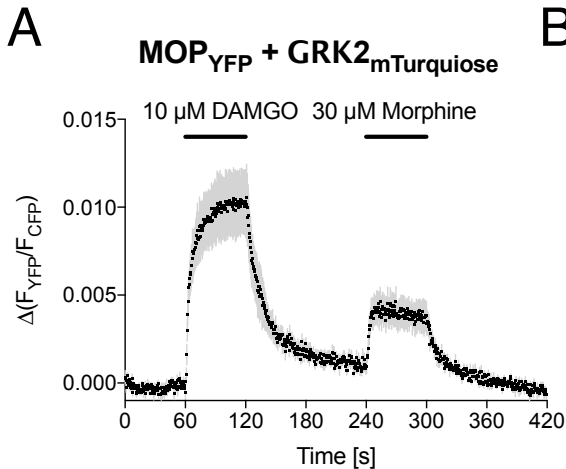


**Figure 6**

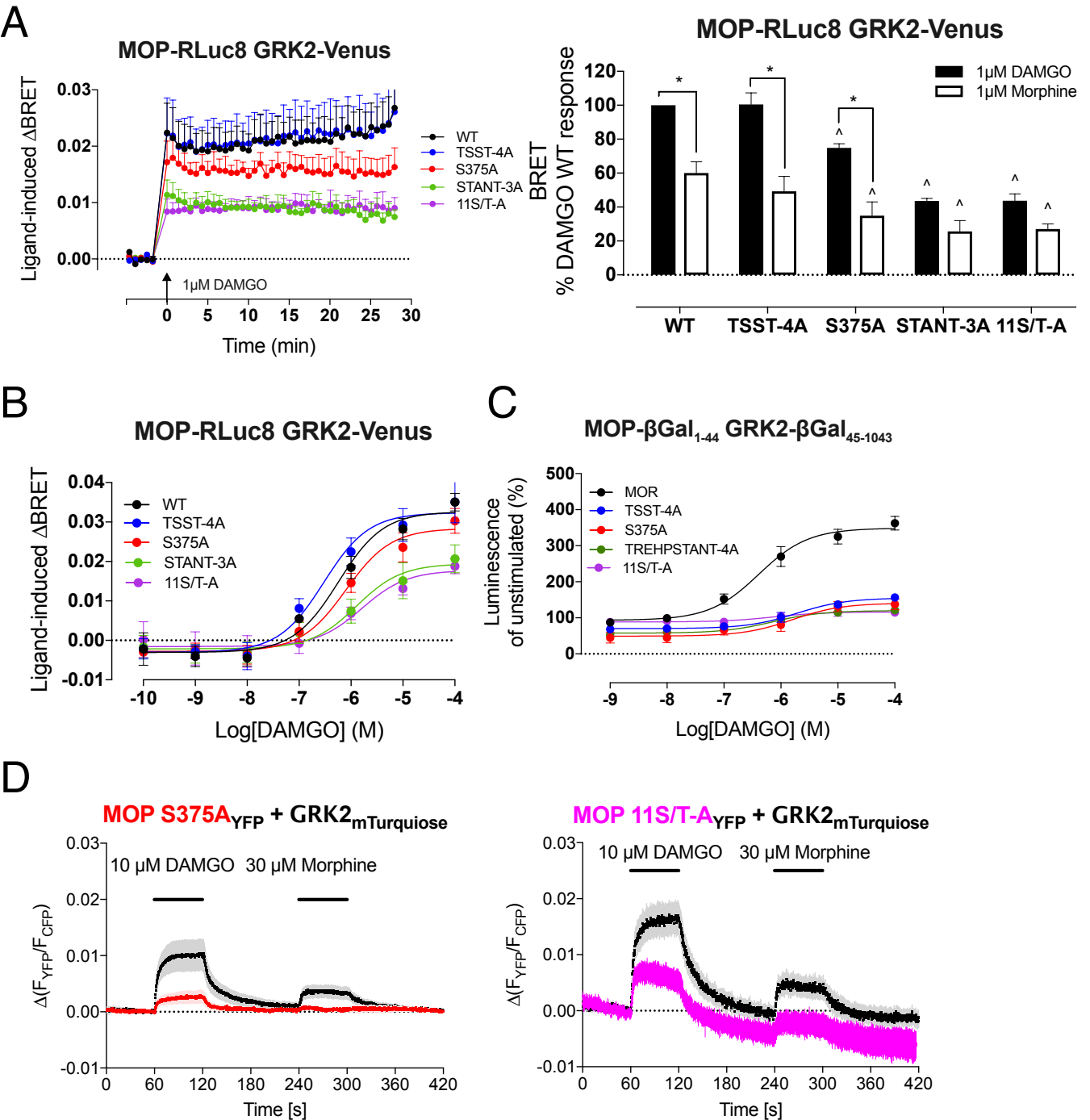


**Figure 7**

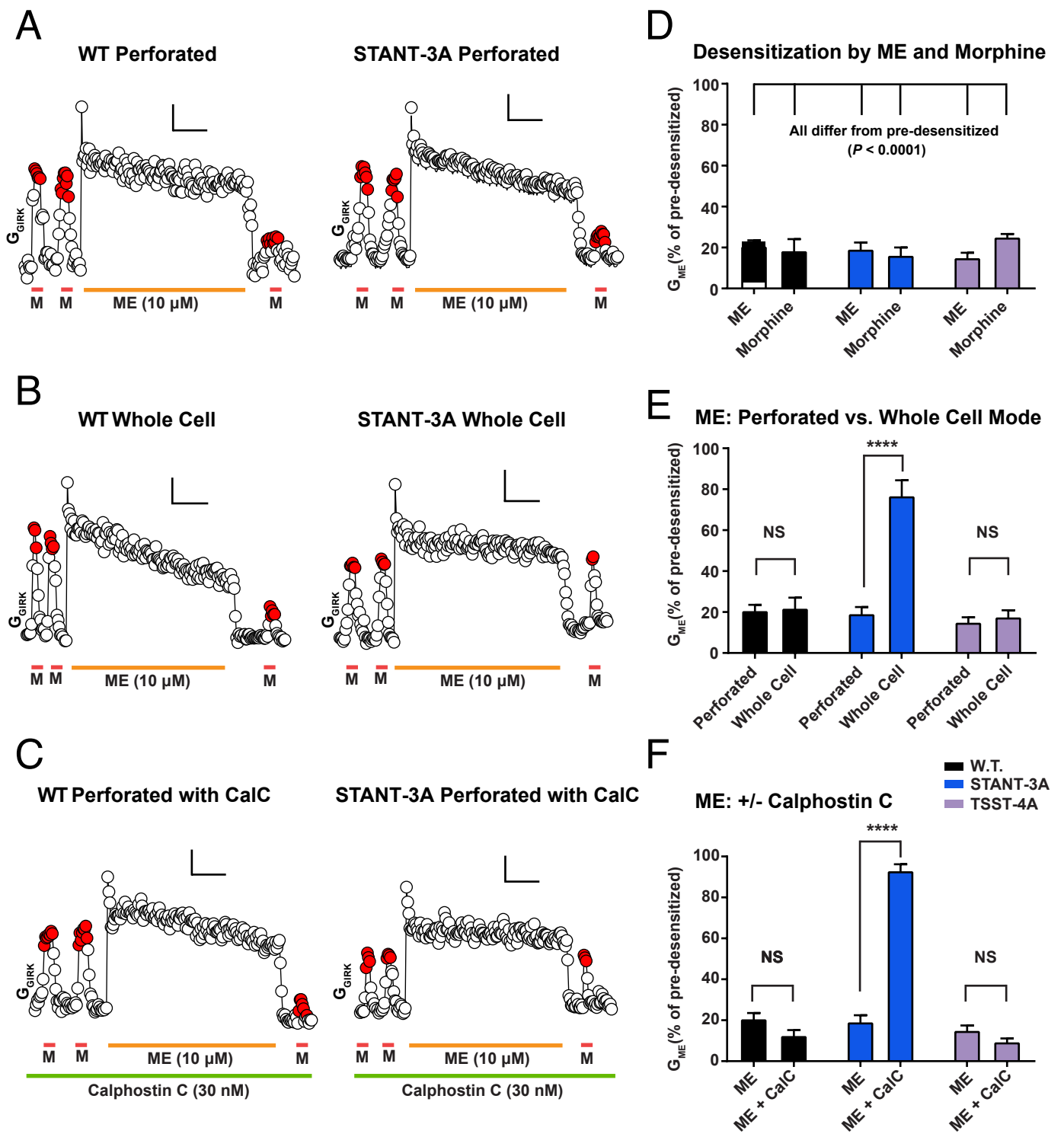


**Figure 8**